




# Modeling and Dynamics Analysis of Zika Transmission with Limited Medical Resources

Hongyong Zhao<sup>1</sup>  · Liping Wang<sup>1</sup> · Sergio Muniz Oliva<sup>2</sup> · Huaiping Zhu<sup>3</sup>

Received: 29 October 2019 / Accepted: 8 July 2020 / Published online: 23 July 2020

© Society for Mathematical Biology 2020

## Abstract

Zika virus, a reemerging mosquito-borne flavivirus, posed a global public health emergency in 2016. Brazil is the most seriously affected country. Some measures have been implemented to control the Zika transmission, such as spraying mosquitoes, developing vaccines and drugs. However, because of the limited medical resources (LMRs) in the country, not every infected patient can be treated in time when infected with Zika virus. We aim to build a deterministic Zika model by introducing a piecewise smooth treatment recovery rate to research the effect of LMRs on the transmission and control of Zika. For the model without treatment, we analyze the global stability of equilibria. For the model with treatment, the model exhibits complex dynamics. We prove that the model with treatment undergoes backward bifurcation, Hopf bifurcation and Bogdanov–Takens bifurcation of codimension 2. It means that the model with LMRs is sensitive to parameters and initial conditions, which has important significance for control of Zika. We also apply the model to estimate the basic and control reproduction numbers for the Zika transmission by using the data on weekly reported accumulated Zika cases from March 25, 2016, to April 14, 2018, in Brazil.

**Keywords** Zika virus · Medical resources · Mosquito-borne and sexual transmission · Backward bifurcation · Hopf bifurcation · Bogdanov–Takens bifurcation

**Mathematics Subject Classification** 34C23 · 34D20 · 34C40

---

✉ Hongyong Zhao  
Hyzho1967@126.com

<sup>1</sup> Department of Mathematics, Nanjing University of Aeronautics and Astronautics, Nanjing 210016, People's Republic of China

<sup>2</sup> Departamento de Matemática Aplicada, Instituto de Matemática e Estatística, Universidade de São Paulo, Rua do Matão, 1010, Cidade Universitária, São Paulo, SP CEP 05508-090, Brazil

<sup>3</sup> Lamps and Department of Mathematics and Statistics, York University, Toronto, ON M3J 1P3, Canada

## 1 Introduction

Zika virus is a reemerging mosquito-borne pathogen initially isolated from rhesus monkeys in the Zika forest, Uganda, in 1947 (Dick et al. 1952). The first case of human infection was reported in Nigeria in 1954 (Dick et al. 1952). The next 50 years, Zika has been quietly circulating in several countries in equatorial Africa and Asia. Few human cases were reported prior to the first recorded outbreak on Yap Island, Micronesia, in April–July 2007 (Duffy 2009). Subsequently, after that in 2013, an outbreak occurred in French Polynesia, with estimated approximately 28,000 infected individuals (Cao-Lormeau and Musso 2014). From then on, Zika virus was not anymore a minor infection restricted to Africa and Asia (Campos et al. 2015; Roa 2016). It has quickly spread to all continents, swept through Central and southern America and arrived in North America in 2016. The widespread of Zika virus urged the World Health Organization (WHO) to declare the outbreak of Zika virus on February 1, 2016, as a “Public Health Emergency of International Concern” (World Health Organization (WHO) 2016).

The mathematical model is a good tool for understanding the mechanisms of interaction between hosts and vectors in depth, going back to Ross (1911) and Macdonald (1952). The first model was used to study transmission dynamics of malaria. For Zika virus, the main transmission vector is *Aedes* species mosquito (*Ae. aegypti* and *Ae. albopictus*) (Marcondes and Ximenes 2016). It is necessary to contain mosquito-borne transmission route into Zika models. Kucharski (2016) employed a compartmental model incorporating both an SEIR (susceptible–exposed–infected–removed) framework for humans and an SEI (susceptible–exposed–infected) framework for vectors to fix the outbreak on the six major islands of French Polynesia between 2013 and 2014 and estimated that 94% of the total population of the six archipelagos were infected during the outbreak. Funk (2016) built the same framework model to study the Zika outbreak on Yap Island, Micronesia, in 2007. In addition, Zika virus may be transmitted via sexual interaction (Musso et al. 2015). Zika models with both sexual and mosquito-borne transmission routes have recently been proposed and analyzed (Gao 2016; Agosto et al. 2017a; Saad-Roy et al. 2018; Sasmal et al. 2018). Dynamics analyses of some various Zika models were obtained (Wang et al. 2017; Agosto et al. 2017a, b; Pizza 2016; Shah et al. 2017; Zhang 2017; Tang et al. 2016; Imran et al. 2017; Wiratsudakul et al. 2018). However, there are very few models to investigate the effects of LMRs on Zika transmission.

Symptoms of Zika infection are generally mild including fever, pain and headache. However, the most frightening thing about Zika virus is that it can interfere with the development of the fetal nervous system, leading to fetal abortion, microcephaly and even stillbirths (Petersen et al. 2016). In addition, Zika virus can cause Guillain–Barré syndrome, myelitis (Schuler-Faccini 2016; Lucchese and Kanduc 2016; Munoz et al. 2016). Due to severe neurological complications caused by Zika virus, the development of anti-Zika drugs is urgently needed, not only to alleviate the virus-induced symptoms, but also to damage the transmission chain. Carolina et al. tested antiviral drug sofosbuvir inhibited the replication of Zika virus (Sacramento et al. 2017). Moreover, sofosbuvir enabled at least 50% (95% confidence interval: 40–60%) of patients to produce significant symptoms decay (Reznik and Ashby 2017). In addi-

tion, 7-deaza-2'-C-methyladenosine was identified as an inhibitor of the replication of Zika virus in vitro and could significantly decrease Zika viremia (Zmurko 2016). Li (2017) tested that 25-hydroxycholesterol could reduce Zika viremia and protect host from Zika virus infection. Except for medicine, there are many factors that determine treatment recovery rate, such as hospital settings, doctors and nurses. For Brazil, the supply of medicines and the number of doctors are far from adequate (Barros et al. 2011; Almeida-Filho 2011). Thus, their medical resources for diagnosis and treatment of patients infected with Zika virus and other mosquito-borne diseases remain still limited.

As of February 2, 2016, approximately 5000 suspected cases of microcephaly were reported, which was 20 times more than in previous years (Arbex et al. 2016). Since Zika case was first reported in the Brazil in May 2015 (Camila et al. 2015), by end of 2016, up to 215,319 reported cases from the Brazil Ministry of Health were identified in Brazil (<http://portalms.saude.gov.br/boletins-epidemiologicos>). According to the "Daily Mail" on February 15, 2016, Goiana, in Pernambuco, Brazil, was the worst place for Zika infection, where at least 40,000 people had been infected and up to 500 new daily infections were sent to already overcrowded hospitals. It has become a great challenge to public health in Brazil (Arbex et al. 2016).

When the Zika infection started in regions of Brazil, the available medical resources of the health system sufficed for diagnosing and treating the infected cases. As the number of infections keeps increasing, the LMRs proved incapable of treating the emerging cases in time. As a result, more susceptible people would be infected via the bite of mosquitoes because of the increasing number of infected humans. Wang and Ruan (2004) first proposed the piecewise treatment function in an SIR model. Later, Wang (2006) improved the treatment function to be proportional to the number of infectious individuals before the capacity of the health system was reached, and otherwise, got the maximal capacity. Shan and Zhu (2014) first introduced the number of hospital beds to the recovery rate. Later, the recovery rate was used in dengue model (Abdelrazec et al. 2016) and Filippov epidemic model (Wang et al. 2018). For the modeling studies of Zika transmission, the study of the effect of LMRs on the control and transmission of Zika is still in its early stages.

The paper is organized as follows. In Sect. 2, we formulate a model for Zika transmission with a non-smooth continuous treatment recovery rate describing the effect of capacity of available medical resources. In addition, the basic properties on the positivity and boundedness of solutions are discussed. In Sect. 3, dynamic behaviors of the model without treatment are analyzed. In Sect. 4, for the model with treatment, we study the existence and stability of equilibria, backward bifurcation, Hopf bifurcation and Bogdanov–Takens bifurcation of codimension 2. For the main results, the biological meaning explanations are given. In Sect. 5, we present numerical simulations to confirm the analytic results. In Sect. 6, the model is applied to mimic the Zika transmission in Brazil. A brief discussion is given in Sect. 7.

## 2 Model Formulation

In this section, we will examine the effect of LMRs on Zika transmission. To this purpose, we formulate a treatment recovery rate depending on LMRs. Denote parameter  $b$  as an indicator to reflect the capacity of available medical resources, which can diagnose and treat maximal number of infective individuals. In fact, when the capacity of medical resources is insufficient, patients infected with Zika virus may take medicine such as acetaminophen to reduce pain and fever. So, the health systems have the lowest medical resources, which can ensure that a certain number of infectious individuals are treated and recovered. That is,  $b$  has down bound, denoted  $\underline{b}$  ( $\underline{b} > 0$ ). Thus,  $b \geq \underline{b}$ .

Based on the discussion in Shan and Zhu (2014), the treatment recovery rate  $\mu$  depends on available medical resources  $b$  and the infectious individuals  $I_h$ . Therefore,  $\mu$  is a function of  $b$  and  $I_h$ . In general, for the treatment recovery rate  $\mu(b, I_h)$ , we extend to have the following assumptions.

- (A1)  $\mu(b, I_h) > 0$  for  $I_h \geq 0, b \geq \underline{b}$ .  $\mu(b, I_h) = \mu_1 > 0$  for  $0 \leq I_h \leq b$ , where  $\mu_1$  is the maximum per capita treatment recovery rate when the capacity of available medical resources is not reached.
- (A2) For fixed parameter  $b \geq \underline{b}$ ,  $\frac{d\mu(b, I_h)}{dI_h} \equiv 0$  for  $0 \leq I_h < b$ , and  $\frac{d\mu(b, I_h)}{dI_h} < 0$  for  $I_h > b$ .  $\lim_{I_h \rightarrow b^+} \mu(b, I_h) = \mu_1$  and  $\lim_{I_h \rightarrow \infty} \mu(b, I_h) = \mu_0 > 0$ . From the assumption (A1), it is obvious that there will be always zero rate of the change of  $\mu$  with respect to  $I_h$  when the capacity of available medical resources is not reached. Once the capacity of available medical resources is reached (i.e.,  $I_h > b$ ),  $\mu(b, I_h)$  is decreasing from  $\mu_1$  and is a decreasing function of  $I_h$ . Moreover, when the number of infectious individuals keeps increasing, the minimum treatment recovery rate  $\mu_0$  can be obtained because the lowest resources can be guaranteed by hospitals.
- (A3) For fixed  $I_h \geq 0$ ,  $\frac{d\mu(b, I_h)}{db} > 0$  for  $\underline{b} \leq b < I_h$ , and  $\frac{d\mu(b, I_h)}{db} \equiv 0$  for  $b > I_h$ .  $\lim_{b \rightarrow \underline{b}} \mu(b, I_h) = \mu_0$  and  $\lim_{b \rightarrow \infty} \mu(b, I_h) = \mu_1$ . The rate of the change of  $\mu$  with respect to  $b$  is the increasing function when the capacity of medical resources is insufficient. From the assumption (A1), if the capacity of medical resources is sufficient, then there will be always zero rate of the change of  $\mu$  with respect to  $b$ . In addition,  $\mu$  is bounded by  $\mu_0$  and  $\mu_1$  for any  $b \geq \underline{b}$ .

In general, based on above assumptions, numerous functional treatment recovery rate can be chosen to satisfy the assumptions. In this paper, we will utilize a simple function as follows:

$$\mu \triangleq \mu(b, I_h) = \begin{cases} \mu_1, & 0 \leq I_h \leq b, \\ \mu_0 + (\mu_1 - \mu_0) \frac{2(b-I_h)}{I_h+b-2\underline{b}}, & I_h > b, \end{cases} \quad (1)$$

which is illustrated in Fig. 1.

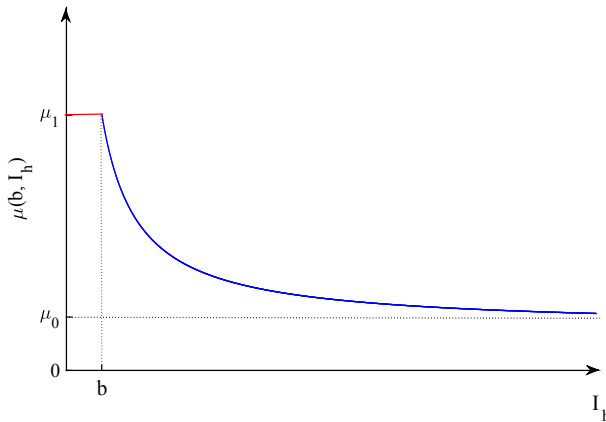


**Fig. 1** The treatment recovery rate  $\mu(b, I_h)$  defined in (1) versus infective individuals  $I_h$  for given  $b$

We rewrite (1) as the non-smooth continuous treatment recovery rate  $\mu(b, I_h)$  as follows:

$$\mu(b, I_h) = \mu_0 + (\mu_1 - \mu_0) \frac{2(b - \underline{b})}{\epsilon I_h + (2 - \epsilon)b - 2\underline{b}}, \quad \epsilon = \begin{cases} 0, & 0 \leq I_h \leq b, \\ 1, & I_h > b. \end{cases} \quad (2)$$

Now, we will study the effect of LMRs on the transmission and control of Zika using the treatment recovery rate (2). Motivated by the compartmental model in Wang et al. (2017), we divide the total number of humans at time  $t$ , denoted by  $N_h(t)$ , into three categories: susceptible humans  $S_h(t)$ , infectious humans  $I_h(t)$  and recovered humans  $R_h(t)$ . So  $N_h(t) = S_h(t) + I_h(t) + R_h(t)$ . We denote the total number of vector mosquitoes at time  $t$  by  $N_v(t)$ , and divide them into two classes: susceptible mosquitoes  $S_v(t)$  and infectious mosquitoes  $I_v(t)$ . That is,  $N_v(t) = S_v(t) + I_v(t)$ . In our work,  $I_h(t)$  indicates symptomatic infectious individuals. The infected individuals mainly take self-recovery and symptomatic treatment.

Susceptible individuals are recruited by birth into the population at a rate  $\Lambda_h$  and may be infected by the Zika virus either via the bite of infectious mosquitoes during biting and feeding at a rate  $a\beta_1 \frac{I_v}{N_h}$  per week or through sexual transmission at a rate  $\beta_3 \frac{I_h}{N_h}$  per week. The infected individuals recover at a natural recovery rate  $r$  per week or a treatment recovery rate  $\mu(b, I_h)$  per week defined by (2). There is a natural death rate of human  $d_h$  per week. Susceptible mosquitoes are recruited at a rate  $\Lambda_v$  and become infectious after biting infectious humans at a rate  $a\beta_2 \frac{I_h}{N_h}$  per week, and later die at a rate  $d_v$  per week. A flow diagram for modeling the transmission of Zika is depicted in Fig. 2. The descriptions of all parameters are shown in Table 1.

Following the flow diagram in Fig. 2, we now adopt the previous models to establish a new model for Zika virus with the non-smooth treatment recovery rate as follows:

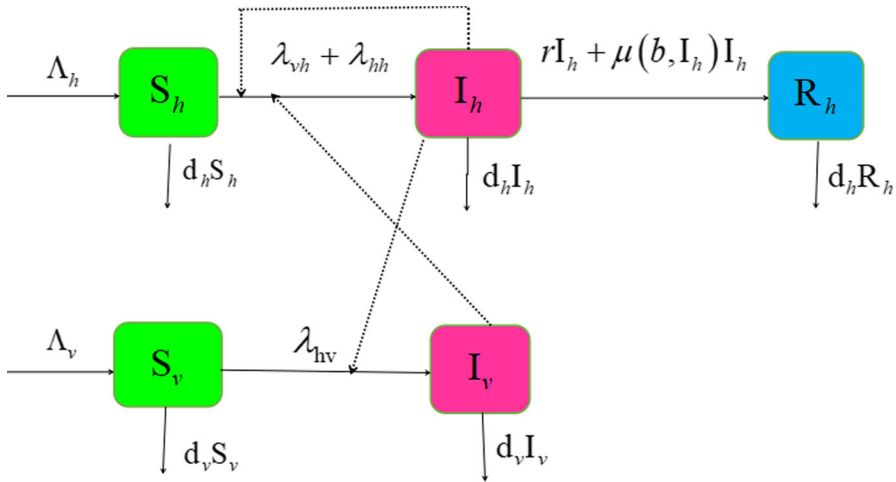


**Fig. 2** Dynamical transmission flow diagram of Zika between humans and mosquitoes. Here,  $\lambda_{vh} = a\beta_1 \frac{S_h I_v}{N_h}$ ,  $\lambda_{hh} = \beta_3 \frac{I_h S_h}{N_h}$ ,  $\lambda_{hv} = a\beta_2 \frac{I_h S_v}{N_h}$ . The parameters are given in Table 1

$$\begin{cases} \frac{dS_h}{dt} = \Lambda_h - a\beta_1 \frac{I_v S_h}{N_h} - \beta_3 \frac{I_h S_h}{N_h} - d_h S_h, \\ \frac{dI_h}{dt} = a\beta_1 \frac{I_v S_h}{N_h} + \beta_3 \frac{I_h S_h}{N_h} - rI_h - \mu(b, I_h)I_h - d_h I_h, \\ \frac{dR_h}{dt} = rI_h + \mu(b, I_h)I_h - d_h R_h, \\ \frac{dS_v}{dt} = \Lambda_v - a\beta_2 \frac{I_h S_v}{N_h} - d_v S_v, \\ \frac{dI_v}{dt} = a\beta_2 \frac{I_h S_v}{N_h} - d_v I_v. \end{cases} \quad (3)$$

The populations of humans and mosquitoes can be confirmed by

$$\frac{dN_h(t)}{dt} = \Lambda_h - d_h N_h(t), \quad \frac{dN_v(t)}{dt} = \Lambda_v - d_v N_v(t),$$

respectively. It is easy to see that for humans and mosquitoes, the corresponding total population sizes are asymptotic constant:  $\lim_{t \rightarrow \infty} N_h(t) = \frac{\Lambda_h}{d_h}$  and  $\lim_{t \rightarrow \infty} N_v(t) = \frac{\Lambda_v}{d_v}$ . Without loss of generality, we can assume  $N_h(t) = \frac{\Lambda_h}{d_h}$  and  $N_v(t) = \frac{\Lambda_v}{d_v}$  for all  $t \geq 0$ . Then,  $\Lambda_h = d_h N_h$  and  $\Lambda_v = d_h N_v$ . Therefore, it suffices to study the following

**Table 1** Parameter descriptions

Parameter	Description
$\Lambda_h$	Recruitment rate of humans ( $\text{week}^{-1}$ )
$\Lambda_v$	Recruitment rate of mosquitoes ( $\text{week}^{-1}$ )
$d_h$	Natural death rate of humans ( $\text{week}^{-1}$ )
$d_v$	Natural death rate of mosquitoes ( $\text{week}^{-1}$ )
$a$	Biting rate of mosquitoes ( $\text{week}^{-1}$ )
$\beta_1$	Transmission probability from infectious mosquitoes to susceptible humans (dimensionless)
$\beta_2$	Transmission probability from infectious humans to susceptible mosquitoes (dimensionless)
$\beta_3$	Sexual transmission rate from infectious humans to susceptible humans ( $\text{week}^{-1}$ )
$r$	Natural recovery rate of humans ( $\text{week}^{-1}$ )
$\mu_0$	Minimum treatment recovery rate of humans ( $\text{week}^{-1}$ )
$\mu_1$	Maximum treatment recovery rate of humans ( $\text{week}^{-1}$ )

system:

$$\begin{cases} \frac{dS_h}{dt} = d_h N_h - a\beta_1 \frac{I_v S_h}{N_h} - \beta_3 \frac{I_h S_h}{N_h} - d_h S_h, \\ \frac{dI_h}{dt} = a\beta_1 \frac{I_v S_h}{N_h} + \beta_3 \frac{I_h S_h}{N_h} - r I_h - \mu(b, I_h) I_h - d_h I_h, \\ \frac{dI_v}{dt} = a\beta_2 \frac{I_h (N_v - I_v)}{N_h} - d_v I_v. \end{cases} \quad (4)$$

The switching system (4) with  $\mu(b, I_h)$  in (2) refers that there is a threshold for infected human  $I_h = b$ .

## 2.1 Basic Property

System (4) describes the interactions between humans and mosquitoes during the Zika epidemic. So, it is epidemiologically significant to study the positivity and boundedness of solutions of system (4).

**Lemma 1** *If initial values  $S_h(0)$ ,  $I_h(0)$ ,  $I_v(0)$  are nonnegative, then the solution  $(S_h(t), I_h(t), I_v(t))$  of system (4) is nonnegative for all  $t \geq 0$ . In particular, the solution  $(S_h(t), I_h(t), I_v(t))$  of system (4) is positive for  $t > 0$  in the existence interval of the solution if  $S_h(0) > 0$ ,  $I_h(0) > 0$ ,  $I_v(0) > 0$ . Moreover, the region  $\Gamma = \{(S_h, I_h, I_v) \mid S_h \geq 0, I_h \geq 0, I_v \geq 0, S_h + I_h \leq \frac{\Lambda_h}{d_h}, I_v \leq \frac{\Lambda_v}{d_h}\}$  is positively invariant with respect to system (4).*

**Proof** It follows from system (4) and  $S_h(0) \geq 0$ ,  $I_h(0) \geq 0$ ,  $I_v(0) \geq 0$  that

$$\begin{aligned} S_h(t) &= S_h(0) \exp \left[ - \int_0^t \left( a\beta_1 \frac{I_v(s)}{N_h} + \beta_3 \frac{I_h(s)}{N_h} \right) ds - d_h t \right] \\ &\quad + d_h N_h \int_0^t \exp \left[ - \int_s^t \left( a\beta_1 \frac{I_v(\xi)}{N_h} + \beta_3 \frac{I_h(\xi)}{N_h} \right) d\xi - d_h(t-s) \right] ds \geq 0, \\ I_v(t) &= I_v(0) \exp \left[ - \int_0^t a\beta_2 \frac{I_h(s)}{N_h} ds - d_v t \right] \\ &\quad + \int_0^t a\beta_2 N_v \frac{I_h(s)}{N_h} \exp \left[ - \int_s^t a\beta_2 \frac{I_h(\xi)}{N_h} d\xi - d_v(t-s) \right] ds \geq 0. \end{aligned}$$

If  $S_h(0) > 0$ ,  $I_v(0) > 0$ , then  $S_h(t) > 0$ ,  $I_v(t) > 0$ . Next, we give that  $I_h(t)$  has the same property under the condition  $I_h(0) > 0$ . Suppose not, then there exists a  $t_1 > 0$  such that  $I_h(t_1) = 0$  and  $I_h(t) > 0$  for  $t \in (0, t_1)$ . Since  $I_h(t_1) = 0$ ,  $S_h(t_1) > 0$ ,  $I_v(t_1) > 0$  and the second equation of (4), we have  $I_h'(t_1) = \frac{a\beta_1 I_v(t_1) S_h(t_1)}{N_h} > 0$ . Thus, there exists a sufficiently small  $\vartheta$  such that  $I_h(t) < 0$  for all  $t \in (t_1 - \vartheta, t_1)$ , which is a contradiction. So,  $I_h(t) > 0$  for  $S_h(0) > 0$ ,  $I_v(0) > 0$ ,  $I_h(0) > 0$ . Adding the first and the second equations of system (4) yields

$$\begin{aligned} \frac{d(S_h + I_h)}{dt} &= d_h N_h - r I_h - \mu(b, I_h) I_h - d_h(S_h + I_h) \\ &\leq d_h N_h - d_h(S_h + I_h), \end{aligned}$$

and we get  $S_h + I_h \leq (S_h(0) + I_h(0))e^{-d_h t} + N_h(1 - e^{-d_h t})$  for  $\forall t \geq 0$ . If  $S_h(0) + I_h(0) \leq N_h$ , then  $S_h + I_h \leq N_h$ .

From the last equation of system (4), we have  $\left. \frac{dI_v}{dt} \right|_{I_v=N_v} = -d_v I_v \leq 0$ . So,  $0 \leq I_v(t) \leq N_v$  for  $I_v(0) \leq N_v$ . Thus,  $\Gamma$  is positively invariant.  $\square$

### 3 Dynamic Analysis Without Treatment

To better analyze the impact of treatment on Zika transmission, we first study dynamic analysis the following model without treatment.

$$\begin{cases} \frac{dS_h}{dt} = \Lambda_h - a\beta_1 \frac{I_v S_h}{N_h} - \beta_3 \frac{I_h S_h}{N_h} - d_h S_h, \\ \frac{dI_h}{dt} = a\beta_1 \frac{I_v S_h}{N_h} + \beta_3 \frac{I_h S_h}{N_h} - r I_h - d_h I_h, \\ \frac{dI_v}{dt} = a\beta_2 \frac{I_h(N_v - I_v)}{N_h} - d_v I_v. \end{cases} \quad (5)$$

It follows from Lemma 1 that  $\Gamma$  is also positively invariant with respect to system (5). System (5) always has a disease-free equilibrium (DFE)  $E_{0w} = (S_{hw}^0, 0, 0)$ ,



where  $S_{hw}^0 = \frac{A_h}{d_h}$ . Calculate the next-generation matrix of system (5) as follows:

$$\begin{aligned} FV^{-1} &= \begin{pmatrix} \frac{\beta_3 S_h^0}{N_h} & \frac{a\beta_1 S_h^0}{N_h} \\ \frac{a\beta_2 N_v}{N_h} & 0 \end{pmatrix} \begin{pmatrix} r+d_h & 0 \\ 0 & d_v \end{pmatrix}^{-1} \\ &= \begin{pmatrix} \frac{\beta_3}{r+d_h} & \frac{a\beta_1}{d_v} \\ \frac{a\beta_2 N_v}{(\mu_1+r+d_h)N_h} & 0 \end{pmatrix}. \end{aligned}$$

Then, the basic reproduction number  $R_0$ , the spectral radius of the next-generation matrix  $FV^{-1}$  in Diekmann et al. (1990) and Van den Driessche and Watmough (2002), is given by

$$R_0 = \frac{R_{hhw} + \sqrt{R_{hhw}^2 + 4R_{hvw}^2}}{2}, \quad (6)$$

where  $R_{hhw} = \frac{\beta_3}{r+d_h}$  is partial reproduction number induced by sexual transmission and  $R_{hvw} = \sqrt{\frac{a^2\beta_1\beta_2 N_v}{d_v N_h(r+d_h)}}$  is partial reproduction number induced by mosquito transmission.

Although the basic reproduction number  $R_0$  is the most important indicator in epidemiology to provide threshold conditions for eradicating an disease, when control is targeted at a specific population rather than at whole population, it is not useful. We are interested in the expected number of secondary infectious humans generated by an infected human. For this purpose, we use the type reproduction number proposed by Roberts and Heesterbeek (2003) and Heesterbeek and Roberts (2007) to describe the meaning above. From Roberts and Heesterbeek (2003) and Heesterbeek and Roberts (2007), we can calculate the type reproduction number of system (5), denoted as  $R_0^*$ , given by

$$\begin{aligned} R_0^* &= e^T K(I - (I - P)K)^{-1} e \\ &= \frac{\beta_3}{r+d_h} + \frac{a^2\beta_1\beta_2 N_v}{d_v N_h(r+d_h)} \\ &= R_{hhw} + R_{hvw}^2, \end{aligned} \quad (7)$$

in which  $K = FV^{-1}$ ,  $e$  represents the first unit vector with the first element to be 1 and others to be 0,  $I$  represents the identity matrix,  $P = (p_{ij})$  represents the projection matrix with  $p_{11} = 1$  and  $p_{ij} = 0$  for other elements. One obtains the following equivalence relations

$$R_0 > 1 \Leftrightarrow R_0^* > 1; R_0 = 1 \Leftrightarrow R_0^* = 1; R_0 < 1 \Leftrightarrow R_0^* < 1.$$

We will use threshold quantity: the type reproduction number of system (5)  $R_0^*$  for the following analysis.

When  $R_0 > 1$ , system (5) has a unique endemic equilibrium, denote  $E_w^* = (S_{hw}^*, I_{hw}^*, I_{vw}^*)$ , in which  $S_{hw}^* = \frac{d_h N_h - (r+d_h)I_{hw}^*}{d_h}$ ,  $I_{vw}^* = \frac{a\beta_2 N_v I_{hw}^*}{a\beta_2 I_{hw}^* + d_v N_h}$ ,  $I_{hw}^* =$

$\frac{-A_1 + \sqrt{A_1^2 - 4A_0A_2}}{2A_0}$ , where

$$\begin{aligned} A_0 &= a\beta_2\beta_3 > 0, \\ A_1 &= d_v N_h(r + d_h)R_0^* + a\beta_2 d_h N_h(1 - R_{hhw}), \\ A_2 &= d_h d_v N_h^2(1 - R_0^*). \end{aligned}$$

**Theorem 1** For system (5), if  $R_0^* < 1$  (or  $R_0 < 1$ ), then  $E_{0w}$  is globally asymptotically stable.

Proof of Theorem 1 is given in “Appendix A”.

**Theorem 2** If  $R_0^* > 1$  (or  $R_0 > 1$ ), then system (5) has a unique globally asymptotically stable endemic equilibrium  $E_w^*$  in  $\Gamma \setminus E_{0w}$ .

Proof of Theorem 2 is given in “Appendix B”.

**Remark 1** Biologically, Theorems 1 and 2 show that the basic reproduction number can be used as a control parameter which determines whether the disease will eventually die out or not. It means that the disease can be eradicated by reducing  $R_0$  below 1.

## 4 Dynamic Analysis for System (4) with Treatment

System (4) always has a disease-free equilibrium (DFE)  $E_0^* = (S_h^0, 0, 0)$ , where  $S_h^0 = N_h$ . When we consider treatment, control measures come into force. Then, the control reproduction number  $R_c$ , by applying the next generation matrix in Diekmann et al. (1990) and Van den Driessche and Watmough (2002), is given by

$$R_c = \rho(FV^{-1}) = \frac{R_{hh} + \sqrt{R_{hh}^2 + 4R_{hv}^2}}{2}, \quad (8)$$

where  $R_{hh} = \frac{\beta_3}{\mu_1 + r + d_h}$  is partial reproduction number induced by sexual transmission and  $R_{hv} = \sqrt{\frac{a^2 \beta_1 \beta_2 N_v}{d_v N_h (\mu_1 + r + d_h)}}$  is partial reproduction number induced by mosquito transmission.

Similar to form (7), we can calculate the type reproduction number of system (4), denoted as  $R_c^*$ , given by

$$R_c^* = R_{hh} + R_{hv}^2.$$

One obtains the following equivalence relations

$$R_c > 1 \Leftrightarrow R_c^* > 1; R_c = 1 \Leftrightarrow R_c^* = 1; R_c < 1 \Leftrightarrow R_c^* < 1. \quad (9)$$

We will use threshold quantity: the type reproduction number of system (4)  $R_c^*$  for the following analysis.

Denote

$$\hat{R}_c^* = \hat{R}_{hh} + \hat{R}_{hv}^2, \quad (10)$$

where  $\hat{R}_{hh} = \frac{\beta_3}{\mu_0 + r + d_h}$  and  $\hat{R}_{hv} = \sqrt{\frac{a^2 \beta_1 \beta_2 N_v}{d_v N_h (\mu_0 + r + d_h)}}$ . Obviously,  $R_c^* < \hat{R}_c^*$ . By analyzing the eigenvalues of the Jacobian matrix of (4) at DFE  $E_0^*$ , we have the following result about the stability of  $E_0^*$ .

**Theorem 3** *The DFE  $E_0^*$  of system (4) is locally asymptotically stable when  $R_c^* < 1$  and unstable when  $R_c^* > 1$ .*

**Proof** The local stability of DFE  $E_0^*$  of system (4) is decided by the eigenvalues of the Jacobian matrix at  $E_0^*$ . Though simple calculations, the eigenvalues of the Jacobian matrix at  $E_0^*$  are  $-d_h$  and the roots of the following function

$$\lambda^2 + (d_v + (\mu_1 + r + d_h)(1 - R_{hh}))\lambda + d_v(\mu_1 + r + d_h)(1 - R_c^*) = 0. \quad (11)$$

If  $R_c^* < 1$ , then  $R_{hh} < 1$ . So, two roots of Eq. (11) have negative real parts. When  $R_c^* > 1$ , Eq. (11) has one positive root. Thus,  $E_0^*$  is locally asymptotically stable when  $R_c^* < 1$  and unstable when  $R_c^* > 1$ .  $\square$

#### 4.1 Existence of the Endemic Equilibria

We consider the following two cases to investigate the existence of the positive equilibrium of system (4).

*Case 1* When  $0 < I_h \leq b$ , an endemic equilibrium of system (4) satisfies

$$\begin{cases} d_h N_h - a\beta_1 \frac{I_v S_h}{N_h} - \beta_3 \frac{I_h S_h}{N_h} - d_h S_h = 0, \\ a\beta_1 \frac{I_v S_h}{N_h} + \beta_3 \frac{I_h S_h}{N_h} - \mu_1 I_h - r I_h - d_h I_h = 0, \\ a\beta_2 \frac{I_h (N_v - I_v)}{N_h} - d_v I_v = 0. \end{cases} \quad (12)$$

Adding the first and second equations of Eq. (12), one can obtain  $S_h = N_h - \frac{(\mu_1 + r + d_h)I_h}{d_h}$  and solve third equation of Eq. (12) to obtain  $I_v = \frac{a\beta_2 N_v I_h}{a\beta_2 I_h + d_v N_h}$ . Substituting them into the second equation of Eq. (12),  $I_h$  satisfies the following equation

$$C_{00}I_h^2 + C_{01}I_h + C_{02} = 0, \quad (13)$$

where  $C_{00} = a\beta_2\beta_3 > 0$ ,  $C_{01} = d_v N_h (\mu_1 + r + d_h)R_c^* + a\beta_2 d_h N_h (1 - R_{hh})$ ,  $C_{02} = d_h d_v N_h^2 (1 - R_c^*)$ .

When  $R_c^* \leq 1$ , clearly,  $C_{02} \geq 0$  and  $C_{01} \geq 0$ . Equation (13) has no positive root. When  $R_c^* > 1$ , that is,  $C_{02} < 0$ . Equation (13) has one positive root  $I_{hf0} = \frac{-C_{01} + \sqrt{\Delta_3}}{2C_{00}}$ , in which  $\Delta_3 = C_{01}^2 - 4C_{00}C_{02}$ . Set  $S_{hf0} = \frac{d_h N_h - (\mu_1 + r + d_h)I_{hf0}}{d_h}$ ,  $I_{vf0} = \frac{a\beta_2 N_v I_{hf0}}{a\beta_2 I_{hf0} + d_v N_h}$ ,

$E_{f0} = (S_{hf0}, I_{hf0}, I_{vf0})$ . Then,  $E_{f0}$  is an endemic equilibrium of system (4) if  $1 < R_c^* \leq 1 + \gamma$ . Here,

$$\gamma = \frac{C_{00}b^2 + C_{01}b}{d_h d_v N_h^2}. \quad (14)$$

*Case 2* When  $I_h > b$ , an endemic equilibrium of system (4) satisfies

$$\begin{cases} d_h N_h - a\beta_1 \frac{I_v S_h}{N_h} - \beta_3 \frac{I_h S_h}{N_h} - d_h S_h = 0, \\ a\beta_1 \frac{I_v S_h}{N_h} + \beta_3 \frac{I_h S_h}{N_h} - (\mu_0 + r + d_h)I_h - (\mu_1 - \mu_0) \frac{2(b - \underline{b})I_h}{I_h + b - 2\underline{b}} = 0, \\ a\beta_2 \frac{I_h(N_v - I_v)}{N_h} - d_v I_v = 0. \end{cases} \quad (15)$$

It follows from Eq. (15) that system (4) has an endemic equilibrium  $\bar{E} = (\bar{S}_h, \bar{I}_h, \bar{I}_v)$ , where  $\bar{S}_h = \frac{1}{d_h}(d_h N_h - (\mu_0 + r + d_h)\bar{I}_h - (\mu_1 - \mu_0) \frac{2(b - \underline{b})\bar{I}_h}{\bar{I}_h + b - 2\underline{b}})$ ,  $\bar{I}_v = \frac{a\beta_2 N_v \bar{I}_h}{a\beta_2 \bar{I}_h + d_v N_h}$ , and  $\bar{I}_h$  satisfies the following equation

$$g(\bar{I}_h) \triangleq D_0 \bar{I}_h^3 + D_1 \bar{I}_h^2 + D_2 \bar{I}_h + D_3 = 0, \quad (16)$$

where

$$\begin{aligned} D_0 &= a\beta_2\beta_3(\mu_0 + r + d_h) > 0, \\ D_1 &= (\beta_3 d_v N_h + a^2\beta_1\beta_2 N_v)(\mu_0 + r + d_h) + a\beta_2\beta_3((\mu_1 + r + d_h)(b - 2\underline{b}) \\ &\quad + b(\mu_1 - \mu_0)) + a\beta_2 d_h N_h(\mu_0 + r + d_h)(1 - \hat{R}_{hh}), \\ D_2 &= (\beta_3 d_v N_h + a^2\beta_1\beta_2 N_v)((\mu_1 + r + d_h)(b - 2\underline{b}) + b(\mu_1 - \mu_0)) \\ &\quad + 2a\beta_2 d_h N_h(\mu_1 - \mu_0)(b - \underline{b}) + a\beta_2(b - 2\underline{b})d_h N_h(\mu_0 + r + d_h)(1 - \hat{R}_{hh}) \\ &\quad + d_h d_v N_h^2(\mu_0 + r + d_h)(1 - \hat{R}_c^*), \\ D_3 &= d_h d_v N_h^2(b - 2\underline{b})(\mu_1 + r + d_h)(1 + \gamma_1 - R_c^*), \end{aligned}$$

in which

$$\gamma_1 = \frac{b(\mu_1 - \mu_0)}{(b - 2\underline{b})(\mu_1 + r + d_h)}. \quad (17)$$

Note that Eq. (16) can have up to three real roots. Further, we analyze the system for the following assumption:

(H1)  $\hat{R}_{hh} < 1$ ,  $b > 2\underline{b}$ . Throughout this work, we assume that (H1) holds. This condition will not be specifically stated below.

Then,  $D_1 > 0$ ,  $\gamma_1 > 0$ . Note that  $R_c^* < 1 + \gamma_1$  if  $D_3 > 0$ .

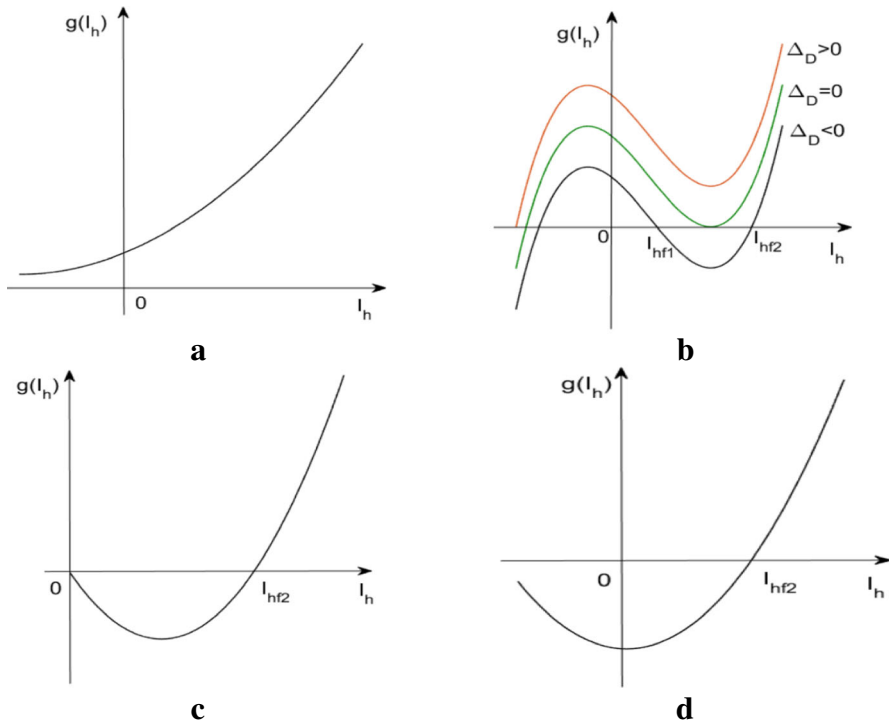


**Fig. 3** The positive roots of  $g(I_h) = 0$ . **a**  $R_c^* < 1 + \gamma_1$ ,  $D_2 > 0$ ; **b**  $R_c^* < 1 + \gamma_1$ ,  $D_2 < 0$ ; **c**  $R_c^* = 1 + \gamma_1$ ,  $D_2 < 0$ ; **d**  $R_c^* > 1 + \gamma_1$ ,  $D_2 = 0$

Next, let

$$A = D_1^2 - 3D_0D_2, \quad B = D_1D_2 - 9D_0D_3, \quad C = D_2^2 - 3D_1D_3.$$

Let  $\Delta_D$  be the discriminant of  $g(I_h)$  with respect to  $I_h$ , then

$$\Delta_D = B^2 - 4AC.$$

From the various possibilities between roots and coefficients and the sign of  $g'(I_h)$  (see in Hu et al. 2012; Li and Zhang 2017), we have the following results:

- Case I*  $D_3 > 0$ . Eq. (16) has no positive solution for  $D_2 \geq 0$  (Fig. 3a). If  $D_2 < 0$ , then we have the following conclusions shown in Fig. 3b:
- (i)  $\Delta_D > 0$ , there are no positive solutions of Eq. (16);
  - (ii)  $\Delta_D \leq 0$ , there are two positive solutions of Eq. (16), denoted as  $I_{hf1}$ ,  $I_{hf2}$ .
- Case II*  $D_3 = 0$ . Eq. (16) has no positive solution for  $D_2 \geq 0$  and has a positive solution for  $D_2 < 0$  (Fig. 3c).
- Case III*  $D_3 < 0$ . It is found that Eq. (16) has a unique positive root, denoted as  $I_{hf2}$ , regardless of the sign of  $D_2$  from Fig. 3d.

Set  $S_{hfi} = \frac{1}{d_h} \left( d_h N_h - (\mu_0 + r + d_h) I_{hfi} - (\mu_1 - \mu_0) \frac{2(b-b)I_{hfi}}{I_{hfi}+b-2b} \right)$ ,  $I_{vfi} = \frac{a\beta_2 N_v I_{hfi}}{a\beta_2 I_{hfi} + d_v N_h}$ ,  $E_{fi} = (S_{hfi}, I_{hfi}, I_{vfi})$  for  $i = 1, 2$ . If  $I_{hfi} > b$ , then  $E_{fi}$  is an endemic equilibrium of (4),  $i = 1, 2$ . Note that  $g(b) = D_0 b^3 + D_1 b^2 + D_2 b + D_3$  and  $g'(b) = 3D_0 b^2 + 2D_1 b + D_2 \triangleq \zeta$ . Solving  $g(b) = 0$  in terms of  $R_c^*$ , one can get  $R_c^* = 1 + \gamma$ . So  $R_c^* < 1 + \gamma$  if  $g(b) > 0$ . To sum up the above discussions, we come to the following conclusions.

**Theorem 4** For system (4) with positive parameters, if (H1) holds, then the following results hold.

- (F1) For  $R_c^* > 1 + \gamma$ , system (4) has a unique endemic equilibrium  $E_{f2}$  if one of the following conditions is satisfied:
  - (i)  $R_c^* > 1 + \gamma_1$ ;
  - (ii)  $R_c^* = 1 + \gamma_1$  and  $D_2 < 0$ ;
  - (iii)  $R_c^* < 1 + \gamma_1$ ,  $D_2 < 0$  and  $\Delta_D < 0$ .
- (F2) For  $R_c^* = 1 + \gamma$ , system (4) has two endemic equilibria  $E_{f0}$  and  $E_{f2}$ , provided that  $R_c^* < 1 + \gamma_1$ ,  $D_2 < 0$ ,  $\Delta_D < 0$ , and  $\zeta < 0$ ; otherwise, system (4) has a unique endemic equilibrium  $E_{f0}$ .
- (F3) For  $1 < R_c^* < 1 + \gamma$ , system (4) has three endemic equilibria  $E_{f0}$ ,  $E_{f1}$  and  $E_{f2}$  if  $R_c^* < 1 + \gamma_1$ ,  $D_2 < 0$ ,  $\Delta_D \leq 0$  and  $\zeta < 0$ ; otherwise, system (4) has a unique endemic equilibrium  $E_{f0}$ .
- (F4) For  $R_c^* = 1$ , system (4) has two endemic equilibria  $E_{f1}$  and  $E_{f2}$  if  $D_2 < 0$ ,  $\Delta_D \leq 0$  and  $\zeta < 0$ ; otherwise, system (4) has no endemic equilibrium.
- (F5) For  $R_c^* < 1$ , and
  - (i) if  $\hat{R}_c^* \leq 1$ , then system (4) has no endemic equilibrium;
  - (ii) if  $\hat{R}_c^* > 1$ , then system (4) has two endemic equilibria  $E_{f1}$  and  $E_{f2}$  of system (4) provided that  $D_2 < 0$ ,  $\Delta_D \leq 0$  and  $\zeta < 0$ ; otherwise, system (4) has no endemic equilibrium.

## 4.2 Stability of Equilibria

From Theorem 4 (F5), for  $R_c^* < 1$ ,  $\hat{R}_c^* > 1$  is a necessary condition for the existence of an endemic equilibrium. If  $\hat{R}_c^* \leq 1$ , then the DFE  $E_0^*$  of system (4) is a unique equilibrium. Next, we will present  $E_0^*$  is also globally asymptotically stable.

**Theorem 5** The DFE  $E_0^*$  of system (4) is the unique equilibrium and globally asymptotically stable in  $\Gamma$  if  $\hat{R}_c^* \leq 1$ .

**Proof** Assume that  $\hat{R}_c^* \leq 1$ . One can easily obtain  $C_{0i} > 0$ ,  $D_j > 0$ ,  $i = 1, 2$ ,  $j = 1, 2, 3$ . Then, Eqs. (13) and (16) have no positive root. Hence, the DFE  $E_0^*$  of system (4) is the unique equilibrium if  $\hat{R}_c^* \leq 1$ .

Consider the Lyapunov functional

$$V = \left( \frac{S_h}{N_h} - \ln \frac{S_h}{N_h} \right) + \frac{I_h}{N_h} + \frac{(\mu_0 + r + d_h)(1 - \hat{R}_{hh})}{a\beta_2} \cdot \frac{I_v}{N_v}$$

in  $\Gamma$ . The orbital derivative of  $V$  along the solution of system (4) can be written as:

$$\begin{aligned} \frac{dV}{dt} \Big|_{(4)} &= \frac{1}{N_h} \left( 1 - \frac{N_h}{S_h} \right) \frac{dS_h}{dt} + \frac{1}{N_h} \frac{dI_h}{dt} + \frac{(\mu_0 + r + d_h - \beta_3)}{a\beta_2 N_v} \frac{dI_v}{dt} \\ &= \frac{1}{N_h} \left( 1 - \frac{N_h}{S_h} \right) \left( d_h N_h - \frac{a\beta_1 S_h I_v}{N_h} - \beta_3 \frac{I_h S_h}{N_h} - d_h S_h \right) \\ &\quad + \frac{a\beta_1 S_h I_v}{N_h^2} + \frac{\beta_3 I_h S_h}{N_h^2} - (\mu_0 + r + d_h) \frac{I_h}{N_h} - \frac{2(b - \underline{b})(\mu_1 - \mu_0)I_h}{(\epsilon I_h + (2 - \epsilon)b - 2\underline{b})N_h} \\ &\quad + \frac{(\mu_0 + r + d_h - \beta_3)}{a\beta_2 N_v} \left( a\beta_2 \frac{I_h(N_v - I_v)}{N_h} - d_v I_v \right) \\ &= -\frac{d_h}{N_h S_h} (N_h - S_h)^2 - (1 - \hat{R}_{hh}) \frac{(\mu_0 + r + d_h)I_v I_h}{N_v N_h} \\ &\quad - \frac{2(b - \underline{b})(\mu_1 - \mu_0)}{\epsilon I_h + (2 - \epsilon)b - 2\underline{b}} \frac{I_h}{N_h} - (1 - \hat{R}_0^*) \frac{d_v(\mu_0 + r + d_h)I_v}{a\beta_2 N_v}. \end{aligned}$$

Then,  $\frac{dV}{dt} \Big|_{(4)} \leq 0$  for  $\hat{R}_0^* \leq 1$ . From the inspection of system (4), it can be seen that  $E_0^*$  is the largest positively invariant set contained in  $\frac{dV}{dt} \Big|_{(4)} = 0$ . Thus, according to the LaSalle theorem,  $E_0^*$  is globally attractive. If  $\hat{R}_c^* \leq 1$ , then  $R_c^* < 1$ . From Theorem 3, we know  $E_0^*$  is locally asymptotically stable. Therefore, the DFE  $E_0^*$  of system (4) is globally stable in  $\Gamma$  for  $\hat{R}_0^* \leq 1$ .  $\square$

In the following, we will present local stability of endemic equilibria by analyzing the eigenvalues of the Jacobian matrix of (4) at endemic equilibria.

**Case 1** When  $0 < I_h < b$ , system (4) has at most a unique endemic equilibrium  $E_{f0}$ . There is the following result for stability of  $E_{f0}$ .

**Theorem 6** For system (4),  $E_{f0}$  is locally asymptotically stable if  $1 < R_c^* < 1 + \gamma$ .

**Proof**  $E_{f0}$  is an endemic equilibrium of (4) under condition  $1 < R_c^* < 1 + \gamma$  from (F3) in Theorem 4. The characteristic equation at  $E_{f0}$  is given by

$$\lambda^3 + \alpha_1 \lambda^2 + \alpha_2 \lambda + \alpha_3 = 0, \quad (18)$$

where

$$\begin{aligned} \alpha_1 &= \frac{\beta_3 I_{hf0}}{N_h} + \frac{a\beta_1 I_{vf0}}{N_h} + d_h + \frac{a\beta_2 I_{hf0}}{N_h} + d_v - \frac{\beta_3 S_{hf0}}{N_h} + \mu_1 + r + d_h, \\ \alpha_2 &= \left( \frac{\beta_3 I_{hf0}}{N_h} + \frac{a\beta_1 I_{vf0}}{N_h} + \frac{a\beta_2 I_{hf0}}{N_h} + d_h \right) \left( -\frac{\beta_3 S_{hf0}}{N_h} + \mu_1 + r + d_h \right) \\ &\quad + \left( \frac{\beta_3 I_{hf0}}{N_h} + \frac{a\beta_1 I_{vf0}}{N_h} + d_h \right) \left( \frac{a\beta_2 I_{hf0}}{N_h} + d_v \right) + \left( \frac{\beta_3 I_{hf0}}{N_h} + \frac{a\beta_1 I_{vf0}}{N_h} \right) \frac{\beta_3 S_{hf0}}{N_h}, \\ \alpha_3 &= \left( \frac{\beta_3 I_{hf0}}{N_h} + \frac{a\beta_1 I_{vf0}}{N_h} + d_h \right) \left( \frac{a\beta_2 I_{hf0}}{N_h} + d_v \right) \left( -\frac{\beta_3 S_{hf0}}{N_h} + \mu_1 + r + d_h \right) \\ &\quad + d_h d_v \left( \frac{\beta_3 S_{hf0}}{N_h} - \mu_1 - r - d_h \right) + \left( \frac{a\beta_2 I_{hf0}}{N_h} + d_v \right) \left( \frac{\beta_3 I_{hf0}}{N_h} + \frac{a\beta_1 I_{vf0}}{N_h} \right) \frac{\beta_3 S_{hf0}}{N_h}. \end{aligned}$$

From the second equation of (12), we can obtain  $-\beta_3 \frac{S_{hf0}}{N_h} + \mu_1 + r + d_h = a\beta_1 \frac{S_{hf0}I_{vf0}}{N_h I_{hf0}} > 0$ . So  $\alpha_1 > 0$ ,  $\alpha_2 > 0$  and  $\alpha_3 > 0$ . It is also easy to verify that

$$\begin{aligned} \alpha_1 \alpha_2 &> \left( \beta_3 \frac{I_{hf0}}{N_h} + a\beta_1 \frac{I_{vf0}}{N_h} + d_h \right) \left( a\beta_2 \frac{I_{hf0}}{N_h} + d_v \right) \left( -\beta_3 \frac{S_{hf0}}{N_h} + \mu_1 + r + d_h \right) \\ &\quad + \beta_3 \left( a\beta_2 \frac{I_{hf0}}{N_h} + d_v \right) \left( \beta_3 \frac{I_{hf0}}{N_h} + a\beta_1 \frac{I_{vf0}}{N_h} \right) \frac{S_{hf0}}{N_h} \\ &> \alpha_3. \end{aligned}$$

Then, the Routh–Hurwitz conditions for Eq. (18) are satisfied. Therefore,  $E_{f0}$  is locally asymptotically stable if  $1 < R_c^* < 1 + \gamma$ .  $\square$

*Case 2* When  $I_h > b$ , let  $E = (S_h, I_h, I_v)$  be any endemic equilibrium, where  $S_h = \frac{1}{d_h} (d_h N_h - (\mu_0 + r + d_h) I_h - (\mu_1 - \mu_0) \frac{2(b-b)I_h}{I_h+b-2b})$ ,  $I_v = \frac{a\beta_2 N_v I_h}{a\beta_2 I_h + d_v N_h}$ . The Jacobian matrix at endemic equilibrium  $E = (S_h, I_h, I_v)$  ( $\bar{E} = E_{f1}$  or  $E = E_{f2}$ ) is given by

$$J_E = \begin{pmatrix} -\beta_3 \frac{I_h}{N_h} - a\beta_1 \frac{I_v}{N_h} - d_h & -\beta_3 \frac{S_h}{N_h} & -\frac{a\beta_1}{N_h} S_h \\ \beta_3 \frac{I_h}{N_h} + a\beta_1 \frac{I_v}{N_h} & \beta_3 \frac{S_h}{N_h} - (r + d_h + \bar{\mu} + \bar{\mu}' I_h) & \frac{a\beta_1}{N_h} S_h \\ 0 & \frac{d_v I_v}{I_h} & -a\beta_2 \frac{I_h^*}{N_h} - d_v \end{pmatrix}. \quad (19)$$

The characteristic equation of Jacobian matrix  $J_E$  is given by

$$\lambda^3 + \bar{\alpha}_1 \lambda^2 + \bar{\alpha}_2 \lambda + \bar{\alpha}_3 = 0, \quad (20)$$

in which

$$\begin{aligned} \bar{\alpha}_1 &= \beta_3 \frac{I_h}{N_h} + a\beta_1 \frac{I_v}{N_h} + r + 2d_h + a\beta_2 \frac{I_h}{N_h} + d_v - \beta_3 \frac{S_h}{N_h} + \bar{\mu} + \bar{\mu}' I_h, \\ \bar{\alpha}_2 &= \left( \beta_3 \frac{I_h}{N_h} + a\beta_1 \frac{I_v}{N_h} + d_h \right) \left( a\beta_2 \frac{I_h}{N_h} + d_v \right) \\ &\quad + \left( \beta_3 \frac{I_h}{N_h} + a\beta_1 \frac{I_v}{N_h} + a\beta_2 \frac{I_h}{N_h} + d_h + d_v \right) (r + d_h + \bar{\mu} + \bar{\mu}' I_h) \\ &\quad + \beta_3 \frac{S_h}{N_h} \left( \beta_3 \frac{I_h}{N_h} + a\beta_1 \frac{I_v}{N_h} \right) - d_v \left( -\beta_3 \frac{S_h}{N_h} + r + d_h + \bar{\mu} \right), \\ \bar{\alpha}_3 &= \left( \beta_3 \frac{I_h}{N_h} + a\beta_1 \frac{I_v}{N_h} + d_h \right) \left( a\beta_2 \frac{I_h}{N_h} + d_v \right) (r + d_h + \bar{\mu} + \bar{\mu}' I_h) \\ &\quad - d_h a \beta_2 \beta_3 \frac{S_h I_h}{N_h^2} - d_h d_v (r + d_h + \bar{\mu}). \end{aligned}$$

Here,  $\bar{\mu} = \mu_0 + \frac{2(b-b)(\mu_1-\mu_0)}{I_h+b-2b}$  and  $\bar{\mu}' \triangleq \frac{d\bar{\mu}}{dI_h} = -\frac{2(b-b)(\mu_1-\mu_0)}{(I_h+b-2b)^2}$ .



From the definition of  $D_i$ ,  $i = 0, 1, 2, 3$ , and Eq. (16), we can represent the coefficient  $\bar{\alpha}_3$  as a function on  $I_h$  as follows:

$$\bar{\alpha}_3(I_h) = \frac{I_h}{N_h^2(I_h + b - 2b)}(g'(I_h)),$$

where  $g(I_h)$  is defined by (16). Obviously, the sign of  $\bar{\alpha}_3(I_h)$  is as same as that  $g'(I_h)$ . It follows from Fig. 3b that  $g'(I_{hf1}) < 0$  and  $g'(I_{hf2}) > 0$  when  $E_{f1}$  and  $E_{f2}$  exist. So  $\bar{\alpha}_3(I_{hf1}) < 0$  and  $\bar{\alpha}_3(I_{hf2}) > 0$ . Thus,  $E_{f1}$  is a saddle and  $E_{f2}$  is an anti-saddle. We know that  $\bar{\alpha}_1(I_{hf2}) > 0$  if (H1) holds. The stability of  $E_{f2}$  depends on the sign of  $\bar{\alpha}_2(I_{hf2})$  and  $\Delta(I_{hf2})$ , where  $\Delta(I_h) = \bar{\alpha}_1(I_h)\bar{\alpha}_2(I_h) - \bar{\alpha}_3(I_h)$ . So we can obtain the following theorem.

**Theorem 7** For system (4), the equilibrium  $E_{f1}$  is a saddle whenever it exists. When the equilibrium  $E_{f2}$  exists and  $\bar{\alpha}_2(I_{hf2}) > 0$ ,  $E_{f2}$  is locally asymptotically stable if  $\Delta(I_{hf2}) > 0$ .

System (4) is non-smooth in  $I_h = b$ . For this case, the stability of equilibrium is analyzed by using a generalized Jacobian matrix in “Appendix C”. From Theorem 7, if  $\Delta(I_{hf2}) = 0$  and  $\bar{\alpha}_2(I_{hf2}) > 0$ , the linearized system of (4) around  $E_{f2}$  has a pair of pure imaginary roots. For this case, we will study it in Sect. 4.3.2. Next, we will first present backward bifurcation analysis.

## 4.3 Bifurcation Analysis

### 4.3.1 Backward Bifurcation

From Theorem 4, we know that when  $R_c^* < 1 + \gamma$ , system (4) may have two epidemic equilibria with  $I_h > b$ . So, system (4) may have a backward bifurcation phenomenon. To verify this, we firstly study the backward bifurcation of the following system:

$$\begin{cases} \frac{dS_h}{dt} = d_h N_h - a\beta_1 \frac{I_v S_h}{N_h} - \beta_3 \frac{I_h S_h}{N_h} - d_h S_h, \\ \frac{dI_h}{dt} = a\beta_1 \frac{I_v S_h}{N_h} + \beta_3 \frac{I_h S_h}{N_h} - (\mu_0 + r + d_h)I_h - (\mu_1 - \mu_0) \frac{2(b-b)I_h}{I_h + b - 2b}, \\ \frac{dI_v}{dt} = a\beta_2 \frac{I_h(N_v - I_v)}{N_h} - d_v I_v, \end{cases} \quad (21)$$

with  $I_h \geq 0$ . It is easy to get that system (21) always has a DFE  $E_0^* = (S_h^0, 0, 0)$ , and the control reproduction number of system (21) is  $\bar{R}_c = \frac{\bar{R}_{hh}}{2} + \frac{\sqrt{\bar{R}_{hh}^2 + 4\bar{R}_{hv}^2}}{2}$ , where  $\bar{R}_{hh} = \frac{\beta_3}{(\mu_1 + r + d_h)(1 + \gamma_1)}$  and  $\bar{R}_{hv} = \sqrt{\frac{a^2 \beta_1 \beta_2 N_v}{d_v N_h (\mu_1 + r + d_h)(1 + \gamma_1)}}$ , in which  $\gamma_1$  is defined by (17). For convenient analysis later, we denote  $\bar{R}_c^* = \bar{R}_{hh} + \bar{R}_{hv}^2$ . One can also obtain the following equivalence relations:

$$\bar{R}_c > 1 \Leftrightarrow \bar{R}_c^* > 1; \bar{R}_c = 1 \Leftrightarrow \bar{R}_c^* = 1; \bar{R}_c < 1 \Leftrightarrow \bar{R}_c^* < 1.$$

Now, we carry out backward bifurcation analysis of system (21) by applying the center manifold theorem (Castillo-Chavez and Song 2004). System (21) can be written in the following form:

$$x' = f(x),$$

with  $x = (x_1, x_2, x_3)^T = (S_h - S_h^0, I_h, I_v)^T$ , and  $f = (f_1, f_2, f_3)^T$  is shown as follows:

$$\begin{cases} f_1 = -a\beta_1 \frac{x_1 x_3}{N_h} - \beta_3 \frac{x_1 x_2}{N_h} - a\beta_1 x_3 - \beta_3 x_2 - d_h x_1, \\ f_2 = a\beta_1 \frac{x_1 x_3}{N_h} + \beta_3 \frac{x_1 x_2}{N_h} + a\beta_1 x_3 + \beta_3 x_2 - (\mu_0 + r + d_h)x_2 \\ \quad - \frac{2(b-\underline{b})(\mu_1 - \mu_0)}{x_2 + b - 2\underline{b}} x_2, \\ f_3 = a\beta_2 \frac{x_2(N_v - x_3)}{N_h} - d_v x_3. \end{cases}$$

Consider  $\bar{R}_c^* = 1$ . Further, choose  $\mu_1$  as the bifurcation parameter. Solving for  $\mu_1$  from  $\bar{R}_c^* = 1$  gives  $\mu_1 = \bar{\mu}_1$ , where

$$\bar{\mu}_1 = \mu_0 + \left( \frac{\beta_3 d_v N_h + a^2 \beta_1 \beta_2 N_v}{d_v N_h} - (\mu_0 + r + d_h) \right) \frac{b - 2\underline{b}}{2(b - \underline{b})}. \quad (22)$$

Let  $\phi = \bar{\mu}_1 - \mu_1$ , then system (21) at the DFE  $E_0^*$  evaluated for  $\phi = 0$  has a simple zero eigenvalue and all other eigenvalues having negative real parts. Hence, the center manifold theorem can be used to analyze the dynamics of (21) near  $\phi = 0$ .

The Jacobian of (21) at  $\phi = 0$ , denoted by  $J(E_0^*)|_{\phi=0}$ , has a right eigenvector (relevant to the zero eigenvalue) given by

$$w = (w_1, w_2, w_3)^T = \left( -\frac{\beta_3 d_v N_h + a^2 \beta_1 \beta_2 N_v}{a \beta_2 d_h N_v}, \frac{d_v N_h}{a \beta_2 N_v}, 1 \right)^T w_3.$$

Similarly, we can obtain a left eigenvector (relevant to the zero eigenvalue) of  $J(E_0^*)|_{\phi=0}$  given by

$$v = (v_1, v_2, v_3) = \left( 0, \frac{d_v}{a \beta_1}, 1 \right) v_3,$$

where  $w_3 > 0$  is required by Theorem 4.1 in Castillo-Chavez and Song (2004). One can choose  $w_3$  and  $v_3$  satisfy  $w_3 v_3 = \frac{a^2 \beta_1 \beta_2 N_v}{d_v^2 N_h + a^2 \beta_1 \beta_2 N_v} > 0$  such that  $v \cdot w = 1$ .

To exhibit the existence of backward bifurcation, we need to calculate second-order partial derivatives of  $f_i$ ,  $i = 1, 2, 3$ , at the DFE  $E_0^*$  and obtain

$$\begin{aligned}\frac{\partial^2 f_1}{\partial x_1 \partial x_2}(0, 0) &= -\frac{\beta_3}{N_h}, \quad \frac{\partial^2 f_1}{\partial x_1 \partial x_3}(0, 0) = -\frac{a\beta_1}{N_h}, \quad \frac{\partial^2 f_2}{\partial x_1 \partial x_2}(0, 0) = \frac{\beta_3}{N_h}, \\ \frac{\partial^2 f_2}{\partial x_1 \partial x_3}(0, 0) &= \frac{a\beta_1}{N_h}, \quad \frac{\partial^2 f_2}{\partial x_2^2}(0, 0) = \frac{4(b - \underline{b})(\bar{\mu}_1 - \mu_0)}{(b - 2\underline{b})^2}, \quad \frac{\partial^2 f_3}{\partial x_2 \partial x_3}(0, 0) = -\frac{a\beta_2}{N_h},\end{aligned}$$

and all other derivatives equal zero.

Now, the coefficients  $\tilde{a}$  and  $\tilde{b}$  defined in Theorem 4.1 in Castillo-Chavez and Song (2004) are calculated as follows:

$$\begin{aligned}\tilde{a} &= \sum_{k,i,j=1}^3 v_k w_i w_j \frac{\partial^2 f_k}{\partial x_i \partial x_j}(0, 0) \\ &= \frac{2}{a^3 \beta_1 \beta_2^2 d_h N_v^2 N_h (b - 2\underline{b})^2} (\bar{b} - b) v_3 w_3^2,\end{aligned}$$

where

$$\bar{b} = \frac{2c_0 \underline{b} + d_v^3 N_h^3 (\bar{\mu}_1 - \mu_0) + (2c_0 \underline{b} d_v^3 N_h^3 (\bar{\mu}_1 - \mu_0) + d_v^6 N_h^6 (\bar{\mu}_1 - \mu_0)^2)^{\frac{1}{2}}}{c_0}, \quad (23)$$

in which  $c_0 = (\beta_3 d_v N_h + a^2 \beta_1 \beta_2 N_v)^2 + a^3 \beta_1 \beta_2^2 d_v N_v N_h$ . In addition, it is easy to show that  $\tilde{b} > 0$ .

So, we obtain  $\tilde{a} > 0$  when  $b < \bar{b}$ . Hence, it follows from Theorem 4.1 of Castillo-Chavez and Song in Castillo-Chavez and Song (2004) that model (21) undergoes backward bifurcation at  $\bar{R}_c^* = 1$  if  $b < \bar{b}$ . Thus, we can obtain the following result.

**Theorem 8** *System (21) undergoes, at  $\bar{R}_c^* = 1$ , a backward bifurcation if  $b < \bar{b}$ , and a forward bifurcation if  $b > \bar{b}$ .*

In this part, we through analyze backward bifurcation of system (21) to represent backward bifurcation phenomenon of system (4). As shown in Fig. 4, system (21) undergoes, at  $\mu_1 = \bar{\mu}_1$  ( $\bar{\mu}_1$  satisfies  $\bar{R}_c^*(\bar{\mu}_1) = 1$ ), a backward bifurcation if  $b < \bar{b}$ . Curves  $C_2$  and  $C_3$  are backward bifurcation curves generated by system (21). We know that when  $I_h > b$ , systems (4) and (21) are identical. So, curves  $C_1$  and  $C_2$  are bifurcation curves generated by system (4). Thus, it follows from Theorems 4 and 8 that system (4) has a backward bifurcation phenomenon if  $b < \bar{b}$ , and the following conditions are satisfied:

$$(i) \Delta_D < 0; \quad (ii) g(b) \geq 0; \quad (iii) g'(b) < 0.$$

Use parameter  $b$  to express the above relations. Firstly, it is too complicated to analysis the curve  $\Delta_D(b) = 0$  analytically. With the help of simulation numerically in Fig. 5, we can present that  $b = b_1$  satisfies  $\Delta_D(b_1) = 0$  and  $\Delta_D < 0$  if and only if  $b < b_1$ .

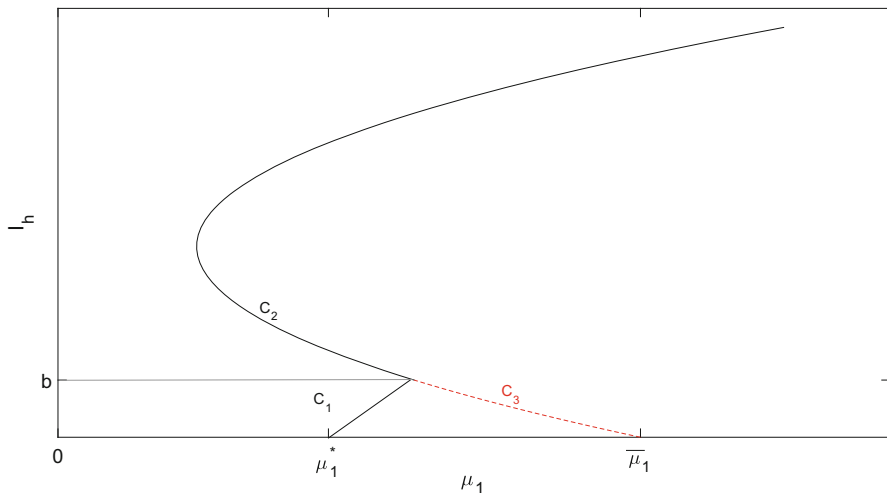


**Fig. 4** Bifurcation diagrams in  $(\mu_1, I_h)$  plane.  $\mu_1^*$  satisfies  $R_c^*(\mu_1^*) = 1$ .  $\bar{\mu}_1$  satisfies  $\bar{R}_c^*(\bar{\mu}_1) = 1$

So condition (i) is equivalent to  $b < b_1$ . Next, if  $g(b) = 0$ , then  $R_c^* = 1 + \gamma$ . Solving  $R_c^* = 1 + \gamma$  for  $b$  gives  $b = b_2$ , where

$$b_2 = \frac{-C_{01} + \sqrt{\Delta_3}}{2C_{00}}, \quad (24)$$

in which  $C_{0i}$  is defined by Eq. (13),  $i = 0, 1, 2$ . We can easily get  $g(b) \geq 0$  (i.e.,  $R_c^* \leq 1 + \gamma$ ) if and only if  $b \geq b_2$ . So condition (ii) is equivalent to  $b \geq b_2$ . Later, since  $g'(b) = 3D_0b^2 + 2D_1b + D_2 = 0$ , we have

$$g'(b) = l_1b^2 + l_2b + l_3 = 0, \quad (25)$$

where

$$\begin{aligned} l_1 &= a\beta_2\beta_3(4\mu_1 + 5r + 5d_h + \mu_0), \\ l_2 &= 2(\beta_3d_vN_h + a^2\beta_1\beta_2N_v)(\mu_0 + r + d_h) - 4a\beta_2\beta_3b(\mu_1 + r + d_h) \\ &\quad + (\beta_3d_vN_h + a^2\beta_1\beta_2N_v + a\beta_2d_hN_h)(2\mu_1 + r + d_h - \mu_0) \\ &\quad + 2a\beta_2d_hN_h(\mu_0 + r + d_h) - 3a\beta_2\beta_3d_hN_h, \\ l_3 &= 2a\beta_2\beta_3d_hN_hb + d_hd_vN_h^2(\mu_0 + r + d_h)(1 - \hat{R}_c^*) \\ &\quad - 2(\mu_1 + r + d_h)(\beta_3d_vN_h + a^2\beta_1\beta_2N_v + a\beta_2d_hN_h)b. \end{aligned}$$

Then, Eq. (25) has unique positive root  $b = b_3$ , where

$$b_3 = \frac{-l_2 + \sqrt{l_2^2 - 4l_1l_3}}{2l_1}. \quad (26)$$

So condition (iii) is equivalent to  $b < b_3$ . Thus, we can obtain the following results.

Similar to the name of bifurcation in Corollary 2.3 in Wang (2006), we also call it as “backward bifurcation with endemic equilibrium.”

**Theorem 9** System (4) undergoes a forward bifurcation with DFE at  $R_c^* = 1$ .

**Theorem 10** For system (4) with positive parameters, the following results hold.

- (B1) When  $b > \bar{b}$ , system (4) does not undergo backward bifurcation.
- (B2) When  $b < \bar{b}$ , system (4) has a backward bifurcation with endemic equilibrium if  $b_2 \leq b < \min\{b_1, b_3\}$ ; otherwise, system (4) does not undergo backward bifurcation.

**Remark 2** Biologically, if  $b < b_2$  or  $b \geq b_3$ , then we can get  $I_h < b$ . That is, the available medical resources suffice for diagnosing and treating the all infected cases. On the other hand,  $b > \bar{b}$  means the available medical resources are rich. For both cases, from Theorems 9 and 10, system (4) does not undergo backward bifurcation. It means that the control reproduction number can be used as a control parameter which determines whether the disease will eventually die out or not. When  $b_2 \leq b < b_1$ , it means that the capacity of the available medical resources is limited; system (4) has a backward bifurcation phenomenon. The disease may not be eradicated by simply lowering control reproduction number below 1 unless it is lowered a new threshold.

Through analyzing the stable of equilibria, there exists a saddle-node bifurcation point  $R_c^{*c}$ .  $R_c^{*c}$  is the new threshold. We can determine  $R_c^{*c}$  by setting  $\Delta_D = 0$ , and we have

$$R_c^{*c} = 1 + \gamma_1 - \gamma_2. \quad (27)$$

where  $\gamma_2 = \frac{18D_0D_1D_2 - 12AD_1 + \sqrt{(18D_0D_1D_2 - 12AD_1)^2 - 324D_0^2D_2^2D_3^2(D_1^2 - 4A)}}{162D_0^2d_hd_vN_h^2(b - 2b)(\mu_1 + r + d_h)}$ . We assume  $1 + \gamma_1 - \gamma_2 > 0$ .

Note that the backward bifurcation is very interesting in application when  $R_c^* < 1$ . We show the following theorem for such a backward bifurcation phenomenon.

**Theorem 11** When  $R_c^{*c} < R_c^* < 1$ , system (4) has a backward bifurcation with endemic equilibrium if  $b < \min\{\bar{b}, b_1, b_3\}$ .

**Remark 3** Biologically, when  $R_c^{*c} < R_c^* < 1$ , a stable DFE coexists with two endemic equilibria. For  $R_c^* < R_c^{*c}$ , system (4) has the unique stable DFE. This indicates that the disease may not be eradicated by simply lowering the value of  $R_c^*$  below 1 unless  $R_c^*$  is lowered a secondary threshold  $R_c^{*c}$ .

#### 4.3.2 Hopf Bifurcation

From Theorem 7, we know that Hopf bifurcation can possibly occur when  $\Delta(I_{hf2}) = 0$  and  $\bar{\alpha}_2(I_{hf2}) > 0$ . If for some value of  $\mu_1$ , denoted  $\mu_1^*$ , we have  $\bar{\alpha}_2(\mu_1^*) > 0$  and

$$\bar{\alpha}_1(\mu_1^*)\bar{\alpha}_2(\mu_1^*) - \bar{\alpha}_3(\mu_1^*) = 0, \quad (28)$$

then the characteristic equation (20) becomes

$$(\lambda + \bar{\alpha}_1(\mu_1^*))(\lambda^2 + \bar{\alpha}_2(\mu_1^*)) = 0, \quad (29)$$

which has a negative real root  $\lambda_1 = -\bar{\alpha}_1(\mu_1^*)$  and a pair of purely imaginary roots  $\lambda_{2,3} = \pm i\sqrt{\bar{\alpha}_2(\mu_1^*)}$ . According to continuity, for sufficiently small  $\epsilon > 0$ , when  $\mu_1 \in (\mu_1^* - \epsilon, \mu_1^* + \epsilon)$ , the eigenvalues are of the form

$$\lambda_1 = -\bar{\alpha}_1(\mu_1), \lambda_2 = w(\mu_1) + iv(\mu_1), \lambda_3 = w(\mu_1) - iv(\mu_1).$$

We need to give the transversality condition to determine whether bifurcation occurs when  $\mu_1 = \mu_1^*$ . By substituting  $\lambda_2$  into Eq. (20), calculating the derivative on  $\mu_1$  and separating the real and imaginary parts, we can get

$$\begin{aligned} Z_1(\mu_1) \frac{dw(\mu_1)}{d\mu_1} - Z_2(\mu_1) \frac{dv(\mu_1)}{d\mu_1} + Z_3(\mu_1) &= 0, \\ Z_2(\mu_1) \frac{dw(\mu_1)}{d\mu_1} - Z_1(\mu_1) \frac{dv(\mu_1)}{d\mu_1} + Z_4(\mu_1) &= 0, \end{aligned}$$

where

$$\begin{aligned} Z_1(\mu_1) &= 3(w^2(\mu_1) - v^2(\mu_1)) + 2\bar{\alpha}_1(\mu_1)w(\mu_1) + \bar{\alpha}_2(\mu_1), \\ Z_2(\mu_1) &= 2\bar{\alpha}_1(\mu_1)v(\mu_1) + 6w(\mu_1)v(\mu_1), \\ Z_3(\mu_1) &= \bar{\alpha}'_3(\mu_1) + \bar{\alpha}'_1(\mu_1)(w^2(\mu_1) - v^2(\mu_1)) + \bar{\alpha}'_2(\mu_1)w(\mu_1), \\ Z_4(\mu_1) &= \bar{\alpha}'_2(\mu_1)v(\mu_1) + 2\bar{\alpha}'_1(\mu_1)w(\mu_1)v(\mu_1). \end{aligned}$$

Solving for  $\frac{dw(\mu_1)}{d\mu_1}$  and setting  $\mu_1 = \mu_1^*$ , we have

$$\left. \frac{dw(\mu_1)}{d\mu_1} \right|_{\mu_1=\mu_1^*} = \left[ \frac{d(\bar{\alpha}_1(\mu_1)\bar{\alpha}_2(\mu_1) - \bar{\alpha}_3(\mu_1))}{d\mu_1} \middle/ (2\bar{\alpha}_1^2(\mu_1) + \bar{\alpha}_2(\mu_1)) \right] \bigg|_{\mu_1=\mu_1^*} \neq 0$$

if  $\left. \frac{d(\bar{\alpha}_1(\mu_1)\bar{\alpha}_2(\mu_1) - \bar{\alpha}_3(\mu_1))}{d\mu_1} \right|_{\mu_1=\mu_1^*} \neq 0$ . It implies from the transversality condition that Hopf bifurcation occurs as  $\mu_1$  crosses the critical value  $\mu_1^*$ . Therefore, we have the following result.

**Theorem 12** *When the equilibrium  $E_{f2}$  exists, if there exists a critical  $\mu_1^*$  of parameter  $\mu_1$  such that  $\bar{\alpha}_2(\mu_1^*) > 0$ ,  $\Delta(\mu_1^*) = 0$  and  $\Delta'(\mu_1^*) \neq 0$  where  $\Delta(\mu_1^*) = \bar{\alpha}_1(\mu_1^*)\bar{\alpha}_2(\mu_1^*) - \bar{\alpha}_3(\mu_1^*)$ , then system (4) undergoes a Hopf bifurcation at  $E_{f2}$  when  $\mu_1$  passes  $\mu_1^*$ .*

Here, we can also choose  $b$  as a bifurcation parameter. If the transversality condition is satisfied, then a similar result can be obtained.

### 4.3.3 Bogdanov–Takens Bifurcation of Codimension 2

We know that when  $R_c^* = R_c^{*c}$ , two endemic equilibria  $E_{f1}$  and  $E_{f2}$  coalesce at the equilibrium  $E^* = (S_h^*, I_h^*, I_v^*)$ , where  $S_h^* = \frac{d_h N_h - (\mu_0 + r + d_h) I_h^* - (\mu_1 - \mu_0) \frac{2(b-b)I_h^*}{I_h^* + b - 2b}}{d_h}$ ,  $I_v^* = \frac{a\beta_2 N_v I_h^*}{a\beta_2 I_h^* + d_v N_h}$ , and  $I_h^*$  is a repeated positive root of Eq. (16). One can get  $\bar{\alpha}_3 = 0$  in Eq. (20) if  $R_c^* = R_c^{*c}$ . If  $\bar{\alpha}_2 = 0$ , the eigenvalues of  $E^*$  are  $\lambda_{1,2} = 0$  and  $\lambda_3 = -\bar{\alpha}_1$ , which suggests that system (4) may undergo a Bogdanov–Takens bifurcation of codimension 2. We confirm this statement by the following theorems.

For convenience later, we note

$$\begin{aligned} m_1 &= r + d_h + \bar{\mu} + \bar{\mu}' I_h^*, \\ m_2 &= \beta_3 \frac{I_h^*}{N_h} + a\beta_1 \frac{I_v^*}{N_h} + d_h, \\ m_3 &= \beta_3 \frac{S_h^*}{N_h}, \\ m_4 &= a\beta_2 \frac{I_h^*}{N_h} + d_v, \\ m_{20} &= \frac{m_1}{d_h} \left( -\frac{m_1 m_4}{d_h} - \frac{m_2^2}{m_2 - d_h} + \bar{\alpha}_1 - m_3 \right) \left( \frac{\beta_3 m_4}{N_h} + \frac{a\beta_1 d_v I_v^*}{N_h I_h^*} \right) \\ &\quad + \left( -\frac{m_1}{d_h} (m_1 + m_2 - m_3) + m_3 + \frac{m_2^2}{m_2 - d_h} \right) \frac{a\beta_2 m_4}{N_h} \\ &\quad + \left( \frac{m_1 m_4}{d_h} + m_3 + \frac{m_2^2}{m_2 - d_h} \right) \frac{2(\mu_1 - \mu_0)(b - \underline{b})(b - 2\underline{b})m_4}{(I_h^* + b - 2\underline{b})^3}, \\ m_{11} &= \frac{1}{d_h^2} \left( -\frac{m_1 m_4}{d_h} - \frac{m_2^2}{m_2 - d_h} + \bar{\alpha}_1 - m_3 \right) (2d_h m_1 + d_h m_4 - m_1 m_4) \frac{\beta_3 m_4}{N_h} \\ &\quad + \left( -\frac{m_1}{d_h} (m_1 + m_2 - m_3) + m_3 + \frac{m_2^2}{m_2 - d_h} \right) \frac{a\beta_2 m_4}{N_h} \\ &\quad + (d_h m_1 + d_h m_4 - m_1 m_4) \frac{a\beta_1 d_v I_v^*}{N_h I_h^*} + \left( \frac{m_1 m_4}{d_h} + m_3 + \frac{m_2^2}{m_2 - d_h} \right) \\ &\quad \times \frac{4(\mu_1 - \mu_0)(b - \underline{b})(b - 2\underline{b})m_4}{(I_h^* + b - 2\underline{b})^3}, \\ l_{20} &= \frac{m_1 m_4}{d_h^3} (d_h m_1 + d_h m_4 - m_1 m_4 - d_h^2) \left( \frac{\beta_3 m_4}{N_h} + \frac{a\beta_1 d_v I_v^*}{N_h I_h^*} \right) \\ &\quad + \frac{1}{d_h^2} (d_h m_1 + d_h m_4 - m_1 m_4) (m_1 + m_2 - m_3) \frac{a\beta_2 m_4}{N_h} \end{aligned}$$

$$\begin{aligned}
& - \left( m_3 + \frac{m_2^2}{m_2 - d_h} \right) \frac{a\beta_2 m_4}{N_h} \\
& - \frac{m_4}{d_h^2} (d_h m_1 + d_h m_4 - m_1 m_4) \frac{2(\mu_1 - \mu_0)(b - \underline{b})(b - 2\underline{b})m_4}{(I_h^* + b - 2\underline{b})^3}.
\end{aligned}$$

**Theorem 13** Suppose  $R_c^* = R_c^{*c}$ ,  $\bar{\alpha}_2(I_h^*) = 0$ ,  $m_{20} \neq 0$  and  $m_{11} + 2l_{20} \neq 0$ . Then, the equilibrium  $E^*$  is a cusp of codimension 2, and system (4) localized at  $E^*$  is topologically equivalent to

$$\begin{cases} \frac{d\eta_1}{dt} = \eta_2, \\ \frac{d\eta_2}{dt} = \frac{d_v I_v^*}{|T|I_h^*} m_{20} \eta_1^2 + \frac{d_v I_v^*}{|T|I_h^*} (m_{11} + 2l_{20}) \eta_1 \eta_2 + \mathcal{O}(|\eta_1, \eta_2|^3), \end{cases} \quad (30)$$

where  $T$  is defined by (44) in “Appendix D”.

The proof is given in “Appendix D”.

System (30) represents the normal form of system (4) restricted to the center manifold at the cusp  $E^*$  of codimension 2. Theorem 13 indicates that system (4) may exhibit Bogdanov–Takens bifurcation of codimension 2. In the following, we discuss if such a bifurcation can be fully unfolded inside the class of system (4) under a small parameter perturbation if the bifurcation parameters are chosen suitably.

$\mu_1$  and  $b$  are chosen as bifurcation parameters to study the Bogdanov–Takens bifurcation of codimension 2 in system (4).  $\mu_1 = \mu_1^o$  and  $b = b^o$  satisfy  $R_c^* = R_c^{*c}$  and  $\bar{\alpha}_2(I_h^*) = 0$ . In order to show  $(\mu_1, b)$  can indeed unfold the cusp type of Bogdanov–Takens bifurcation of codimension 2, we perturb the parameters  $(\mu_1, b)$  in the small neighborhood of  $(\mu_1^o, b^o)$  in system (4). Thus, we let  $\mu_1 = \mu_1^o + \epsilon_1$  and  $b = b^o + \epsilon_2$ , where  $\epsilon = (\epsilon_1, \epsilon_2)$  is a parameter vector in a small neighborhood of  $(0, 0)$ . Next, we study the bifurcations of the following system using  $(\epsilon_1, \epsilon_2)$  as bifurcation parameters

$$\begin{cases} \frac{dS_h}{dt} = d_h N_h - a\beta_1 \frac{I_v S_h}{N_h} - \beta_3 \frac{I_h S_h}{N_h} - d_h S_h, \\ \frac{dI_h}{dt} = a\beta_1 \frac{I_v S_h}{N_h} + \beta_3 \frac{I_h S_h}{N_h} - (\mu_0 + r + d_h) I_h \\ \quad - (\mu_1^o + \epsilon_1 - \mu_0) \frac{2(b^o + \epsilon_2 - \underline{b}) I_h}{I_h + b^o + \epsilon_2 - 2\underline{b}}, \\ \frac{dI_v}{dt} = a\beta_2 \frac{I_h (N_v - I_v)}{N_h} - d_v I_v. \end{cases} \quad (31)$$

For convenience, we note

$$\begin{aligned}
q_1(\epsilon) &= \frac{2(b^o - \underline{b})(\mu_1^o - \mu_0)}{I_h^* + b^o - 2\underline{b}} - \frac{2(b^o + \epsilon_2 - \underline{b})(\mu_1^o - \mu_0 + \epsilon_1)}{I_h^* + b^o + \epsilon_2 - 2\underline{b}}, \\
q_2(\epsilon) &= \frac{2(b^o - \underline{b})(b^o - 2\underline{b})(\mu_1^o - \mu_0)}{(I_h^* + b^o - 2\underline{b})^2}
\end{aligned}$$



$$q_3(\epsilon) = \frac{2(b^o + \epsilon_2 - \underline{b})(b^o + \epsilon_2 - 2\underline{b})(\mu_1^o - \mu_0 + \epsilon_1)}{(I_h^* + b^o + \epsilon_2 - 2\underline{b})^2} - \frac{2(b^o - \underline{b})(b^o - 2\underline{b})(\mu_1^o - \mu_0)}{(I_h^* + b^o - 2\underline{b})^3} - \frac{2(b^o + \epsilon_2 - \underline{b})(b^o + \epsilon_2 - 2\underline{b})(\mu_1^o - \mu_0 + \epsilon_1)}{(I_h^* + b^o + \epsilon_2 - 2\underline{b})^3}.$$

If we repeat the similar procedure of applying the transmission (45) and reducing to the center manifold, then system (31) takes the form

$$\begin{cases} \frac{du_1}{dt} = u_2 + a_{00}(\epsilon) + a_{10}(\epsilon)u_1 + a_{01}(\epsilon)u_2 + \frac{1}{2}a_{20}(\epsilon)u_1^2 \\ \quad + a_{11}(\epsilon)u_1u_2 + \frac{1}{2}a_{02}(\epsilon)u_2^2 + \mathcal{O}(|u_1, u_2|^3), \\ \frac{du_2}{dt} = b_{00}(\epsilon) + b_{10}(\epsilon)u_1 + b_{01}(\epsilon)u_2 + \frac{1}{2}b_{20}(\epsilon)u_1^2 \\ \quad + b_{11}(\epsilon)u_1u_2 + \frac{1}{2}b_{02}(\epsilon)u_2^2 + \mathcal{O}(|u_1, u_2|^3), \end{cases} \quad (32)$$

where

$$a_{00}(\epsilon) = -\frac{d_v I_v^*}{|T|d_h^2}(d_h m_1 + d_h m_4 - m_1 m_4)q_1(\epsilon),$$

$$a_{10}(\epsilon) = -\frac{d_v I_v^* m_4}{|T|d_h^2 I_h^*}(d_h m_1 + d_h m_4 - m_1 m_4)q_2(\epsilon),$$

$$a_{01}(\epsilon) = \frac{1}{m_4}a_{10}(\epsilon),$$

$$b_{00}(\epsilon) = \frac{d_v I_v^*}{|T|} \left( \frac{m_1 m_4}{d_h} + m_3 + \frac{m_2^2}{m_2 - d_h} \right) q_1(\epsilon),$$

$$b_{10}(\epsilon) = \frac{d_v I_v^* m_4}{|T|I_h^*} \left( \frac{m_1 m_4}{d_h} + m_3 + \frac{m_2^2}{m_2 - d_h} \right) q_2(\epsilon),$$

$$b_{01}(\epsilon) = \frac{1}{m_4}b_{10}(\epsilon),$$

$$a_{20} = 2L_{20} + \frac{2d_v I_v^*}{|T|d_h^2 I_h^*}(d_h m_1 + d_h m_4 - m_1 m_4) \left( m_4^2 q_3(\epsilon) - s_0(m_1 + m_2 - m_3)q_2(\epsilon) \right),$$

$$a_{11} = L_{11} + \frac{d_v I_v^*}{|T|d_h^2 I_h^*}(d_h m_1 + d_h m_4 - m_1 m_4) (2m_4 q_3(\epsilon) - s_1(m_1 + m_2 - m_3)q_2(\epsilon)),$$

$$a_{02} = 2L_{02} + \frac{2d_v I_v^*}{|T|d_h^2 I_h^*}(d_h m_1 + d_h m_4 - m_1 m_4) (q_3(\epsilon) - s_2(m_1 + m_2 - m_3)q_2(\epsilon)),$$

$$\begin{aligned}
b_{20} &= 2M_{20} - \frac{2d_v I_v^*}{|T|I_h^*} \left( \frac{m_1 m_4}{d_h} + m_3 + \frac{m_2^2}{m_2 - d_h} \right) (m_4^2 q_3(\epsilon)) \\
&\quad - s_0(m_1 + m_2 - m_3)q_2(\epsilon), \\
b_{11} &= M_{11} - \frac{d_v I_v^*}{|T|I_h^*} \left( \frac{m_1 m_4}{d_h} + m_3 + \frac{m_2^2}{m_2 - d_h} \right) (2m_4 q_3(\epsilon)) \\
&\quad - s_1(m_1 + m_2 - m_3)q_2(\epsilon), \\
b_{02} &= 2M_{02} - \frac{2d_v I_v^*}{|T|I_h^*} \left( \frac{m_1 m_4}{d_h} + m_3 + \frac{m_2^2}{m_2 - d_h} \right) (q_3(\epsilon)) \\
&\quad - s_2(m_1 + m_2 - m_3)q_2(\epsilon).
\end{aligned}$$

To make the calculations easier, we will remove  $\epsilon$  from the expressions  $a_{ij}(\epsilon)$  and  $b_{ij}(\epsilon)$  (i.e.,  $a_{ij} = a_{ij}(\epsilon)$  and  $b_{ij} = b_{ij}(\epsilon)$ ),  $i, j = 0, 1, 2$ . Making transmission

$$\begin{aligned}
X &= u_1, \quad Y = u_2 + c_{00} + c_{10}u_1 + c_{01}u_2 + \frac{1}{2}c_{20}u_1^2 + c_{11}u_1u_2 + \frac{1}{2}c_{02}u_2^2 \\
&\quad + \mathcal{O}(|u_1, u_2|^3),
\end{aligned}$$

system (32) becomes

$$\begin{cases} \frac{dX}{dt} = Y, \\ \frac{dY}{dt} = g_{00} + g_{10}X + g_{01}Y + \frac{1}{2}g_{20}X^2 + g_{11}XY + \frac{1}{2}g_{02}Y^2 + \mathcal{O}(|X, Y|^3), \end{cases} \quad (33)$$

where

$$\begin{aligned}
g_{00} &= b_{00} - a_{00}b_{01} + \frac{1}{2}b_{02}a_{00}^2 + a_{01}b_{00} - a_{00}a_{01}b_{01} + \frac{1}{2}a_{01}b_{02}a_{00}^2 - a_{00}b_{00}a_{02} \\
&\quad + b_{01}a_{02}a_{00}^2, \\
g_{10} &= b_{10} - a_{10}b_{01} - a_{00}b_{11} + a_{00}a_{10}b_{02} + a_{01}b_{01} - a_{10}a_{01}b_{01} - a_{00}a_{01}b_{11} \\
&\quad + a_{00}a_{10}a_{01}b_{02} + b_{00}a_{11} - a_{00}b_{01}a_{11} + \frac{1}{2}a_{00}^2b_{02}a_{11} - a_{10}b_{00}a_{02} - a_{00}b_{10}a_{02} \\
&\quad + 2a_{00}a_{10}b_{01}a_{02} + b_{11}a_{02}a_{00}^2, \\
g_{01} &= b_{01} - a_{00}b_{02} + a_{10} + a_{01}b_{01} - a_{00}a_{01}b_{02} - a_{00}a_{11} + b_{00}a_{02} - 2a_{00}b_{01}a_{02}, \\
g_{20} &= b_{20} - 2a_{10}b_{11} + a_{10}^2b_{02} + a_{01}b_{20} - 2a_{10}a_{01}b_{11} - 2a_{00}b_{11}a_{11} + 2a_{00}a_{10}a_{11}b_{02} \\
&\quad - 2a_{10}b_{10}a_{02} + 2a_{10}^2b_{01}a_{02} - \frac{1}{2}a_{00}b_{20}a_{02} + 4a_{00}a_{10}b_{11}a_{02}, \\
g_{11} &= b_{11} - a_{10}b_{02} + a_{01}b_{11} - a_{10}a_{01}b_{02} + a_{20} + b_{01}a_{11} - a_{00}b_{02}a_{11} - a_{10}a_{11} \\
&\quad + b_{10}a_{02} - 2a_{10}b_{01}a_{02} - 2a_{00}b_{11}a_{02} \text{ and} \\
g_{02} &= b_{02} + a_{01}b_{02} + 2a_{11} + 2b_{01}a_{02}.
\end{aligned}$$

One can verify  $g_{00}(0) = g_{10}(0) = g_{01}(0) = 0$ ,  $g_{20}(0) = b_{20}(0)$ ,  $g_{02}(0) = b_{02}(0) + 2a_{11}(0)$ ,  $g_{11}(0) = b_{11}(0) + a_{20}(0) = M_{11} + 2L_{20} = \frac{d_v I_v^*}{|T|I_h^*}(m_{11} + 2l_{20}) \neq 0$ .

Taking transmission  $X = v_1 - \frac{g_{01}(\epsilon)}{g_{11}(0)}$ ,  $Y = v_2$ , system (33) becomes

$$\begin{cases} \frac{dv_1}{dt} = v_2, \\ \frac{dv_2}{dt} = h_{00} + h_{10}v_1 + \frac{1}{2}h_{20}v_1^2 + h_{11}v_1v_2 + \frac{1}{2}h_{02}v_2^2 + \mathcal{O}(|v_1, v_2|^3), \end{cases} \quad (34)$$

where

$$\begin{aligned} h_{00} &= h_{00}(\epsilon) = g_{00}(\epsilon) - \frac{g_{01}(\epsilon)}{g_{11}(0)}g_{10}(\epsilon) + \mathcal{O}(\delta^2), \quad h_{20} = h_{20}(\epsilon) = g_{20} + \mathcal{O}(\delta), \\ h_{10} &= h_{10}(\epsilon) = g_{10}(\epsilon) - \frac{g_{01}(\epsilon)}{g_{11}(0)}g_{20}(\epsilon) + \mathcal{O}(\delta^2), \quad h_{11} = h_{11}(\epsilon) = g_{11} + \mathcal{O}(\delta), \\ h_{02} &= h_{02}(\epsilon) = g_{02} + \mathcal{O}(\delta), \\ \text{in which } \delta &= \frac{g_{01}(\epsilon)}{g_{11}(0)}. \end{aligned}$$

Introducing a new time variable  $\tau$  by  $dt = \left(1 - \frac{h_{02}(\epsilon)}{2}v_1\right) d\tau$  and rewriting  $\tau$  as  $t$ , we can get

$$\begin{cases} \frac{dv_1}{dt} = v_2 - \frac{h_{02}(\epsilon)}{2}v_1v_2, \\ \frac{dv_2}{dt} = h_{00} + \left(h_{10} - \frac{h_{02}}{2}h_{00}\right)v_1 + \frac{1}{2}\left(h_{20} - 2\frac{h_{02}}{2}h_{10}\right)v_1^2 \\ \quad + h_{11}v_1v_2 + \frac{1}{2}h_{02}v_2^2 + \mathcal{O}(|v_1, v_2|^3). \end{cases} \quad (35)$$

Let  $\xi_1 = v_1$ ,  $\xi_2 = v_2 - \frac{h_{02}(\epsilon)}{2}v_1v_2$ , then (35) becomes

$$\begin{cases} \frac{d\xi_1}{dt} = \xi_2, \\ \frac{d\xi_2}{dt} = q_{00} + q_{10}\xi_1 + q_{20}\xi_1^2 + q_{11}\xi_1\xi_2 + \mathcal{O}(|\xi_1, \xi_2|^3), \end{cases} \quad (36)$$

where  $q_{00} = h_{00}$ ,  $q_{10} = h_{10} - h_{00}h_{02}$ ,  $q_{20} = \frac{1}{2}(h_{20} - 2h_{10}h_{02} + \frac{1}{2}h_{00}h_{02}^2)$ ,  $q_{11} = h_{11}$ .

By simple calculation, we show that  $q_{00}(0) = q_{10}(0) = 0$ ,  $q_{20}(0) = \frac{d_v I_v^*}{|T|I_h^*}m_{20} \neq 0$ ,  $q_{11}(0) = \frac{d_v I_v^*}{|T|I_h^*}(m_{11} + 2l_{20}) \neq 0$ . If  $\epsilon = 0$ , then system (36) becomes (30). By introducing the change of variables and rescaling of time

$$\eta_1 = \frac{q_{11}^2}{q_{20}}\xi_1, \quad \eta_2 = \text{sign}\left(\frac{q_{20}}{q_{11}}\right)\frac{q_{11}^3}{q_{20}^2}\xi_2, \quad t = \left|\frac{q_{20}}{q_{11}}\right|\tau$$

in a small neighborhood of the original point and renaming  $\tau$  as  $t$ , system (36) becomes

$$\begin{cases} \frac{d\eta_1}{dt} = \eta_2, \\ \frac{d\eta_2}{dt} = \rho_1 + \rho_2\eta_1 + \eta_1^2 + s\eta_1\eta_2 + \mathcal{O}(|\eta_1, \eta_2|^3), \end{cases} \quad (37)$$

where  $\rho_1 = \frac{q_{00}q_{11}^4}{q_{20}^3}$ ,  $\rho_2 = \frac{q_{10}q_{11}^2}{q_{20}^2}$ ,  $s = \text{sign}\left(\frac{q_{20}(0)}{q_{11}(0)}\right)$ .

By the results in Kuznetsov (1995), system (37) is the versatile unfolding of the Bogdanov–Takens singularity of codimension 2, and the dynamics of system (4) in a small neighborhood of the equilibrium  $E^*$  as  $(\mu_1, b)$  varying near  $(\mu_1^o, b^o)$  are equivalent to that of system (37) in a small neighborhood of  $(0, 0)$  as  $(\rho_1, \rho_2)$  varying near  $(0, 0)$ . We also obtain the following local expressions of the bifurcation curves in a small neighborhood of  $E^*$ .

**Theorem 14** *Under the conditions of Theorem 13, system (4) undergoes a Bogdanov–Takens bifurcation of codimension 2. If we use  $\mu_1$  and  $b$  as bifurcation parameters, the bifurcation cures are given by the following:*

(I) *there is a saddle-node bifurcation curve*

$$\text{SN} = \left\{ (\mu_1 - \mu_1^o, b - b^o) : 4\rho_1 = \rho_2^2 \right\};$$

(II) *there is a Hopf bifurcation curve*

$$\text{Hopf} = \left\{ (\mu_1 - \mu_1^o, b - b^o) : \rho_1 = 0, \rho_2 < 0 \right\};$$

(III) *there is a homoclinic bifurcation curve*

$$\text{Hom} = \left\{ (\mu_1 - \mu_1^o, b - b^o) : 25\rho_1 + 6\rho_2^2 = o(\rho_2^2), \rho_2 < 0 \right\}.$$

**Remark 4** Biologically, the Bogdanov–Takens bifurcation of codimension 2 is found, which shows that trends of Zika epidemic with the limited medical resources can be revealed in several different parameter regions. The saddle-node bifurcation, Hopf bifurcation and homoclinic bifurcation will occur. It means that there are rich behaviors for trends of Zika epidemic, such as extinction, multiple stable or epidemic break out in periodic pattern. Thus, trends of Zika epidemic are sensitive as parameter vector  $(\mu_1, b)$  perturbs in the small neighborhood of  $(\mu_1^o, b^o)$ .

**Remark 5** It is not easy to give an explicit determination of the sign of  $m_{20}$  and  $(m_{11} + 2l_{20})$  due to the complexity involved. We observe from simulations that  $m_{20}$  and  $(m_{11} + 2l_{20})$  can have alternate signs or vanish which suggest higher co-dimension bifurcation may occur. Therefore, we leave the cases when  $m_{20}$  or  $(m_{11} + 2l_{20}) = 0$  for future work.

**Table 2** Parameter descriptions

Parameter	Range	Value	References
$a$	(2.1, 7)	2.1	Andraud et al. (2011)
$\beta_1$	(0, 0.97)	0.015	Zhang (2017)
$\beta_2$	(0, 0.97)	0.3	Zhang (2017)
$\beta_3$	(0.001, 0.1)	0.08	Gao (2016)
$r$	$\left(\frac{7}{30}, \frac{7}{2}\right)$	$\frac{7}{25}$	Gourinat et al. (2015) and Froeschl (2017)
$\mu_0$	( $r$ , 1)	0.5	Assumption
$d_h$		$\frac{1}{75 \times 52}$	Wiratsudakul et al. (2018)
$N_h$		$2.05 \times 10^8$	<a href="http://population.city/brazil/#cities">http://population.city/brazil/#cities</a>
$N_v$	( $2.05 \times 10^8$ , $2.05 \times 10^9$ )	$3 \times 10^8$	Wang et al. (2017)
$d_v$	$\left(\frac{7}{50}, \frac{7}{4}\right)$	0.04075	Andraud et al. (2011)

## 5 Numerical Simulations

Using numerical computations, bifurcation diagrams and numerical simulations of system (4) are provided to substantiate the theoretical results.

### 5.1 Bifurcation Diagram in $(\mu_1, b)$ Plane

According to the above analyses, we know that system (4) can undergo Bogdanov–Takens bifurcation of codimension 2. In this subsection, the parameters  $\mu_1$  and  $b$  are chosen as bifurcation parameters to present bifurcation diagram.

Fixing all parameters in Table 2 except  $\mu_1$  and  $b$ , choosing  $\underline{b} = 30$ , we get  $\frac{1}{|T|}(m_{11} + 2l_{20}) > 0$  and  $BT^+ = (\mu_1^o, b^o) = (0.51012, 255)$  satisfying the conditions in Theorem 13 ( $BT^+$  represents the positive coefficient of  $\eta_1\eta_2$  term in the normal form (30)).  $E^* = (2.037 \times 10^8, 425, 9725)$  is the Bogdanov–Takens point of order 2. By simulation, we plot three bifurcation curves in Theorem 14 in  $(\mu_1, b)$  plane shown in Fig. 5 and the phase portrait of (4) at  $BT^+$  shown in Fig. 6. In Fig. 5, the blue solid curve represents saddle-node bifurcation (SN), the red solid curve represents subcritical Hopf bifurcation (Hopf) and the green solid curve represents homoclinic bifurcation (Hom). The curve Hom and curve Hopf are tangent to curve SN and end at  $BT^+$ . The SN curve is separated into two parts by  $BT^+$  point. Its upper part is the attracting saddle-node curve  $SN^-$  connecting to the attracting hyperbolic node point ( $L_0$ ), and its lower part extending to infinity is the repelling saddle-node curve  $SN^+$ . Between the curve Hopf and curve Hom, there is only one unstable limit cycle. Next, we give other bifurcation curves.

It is easy to get  $L^*$ :  $\mu_1 = \frac{a^2\beta_1\beta_2N_v}{d_vN_h} + \beta_3 - (r + d_h) \triangleq \mu_1^1$  by solving  $R_c^* = 1$ . The forward bifurcation at DFE occurs on the line  $L^*$ . Curve  $L$ :  $b = b_2(\mu_1)$  is

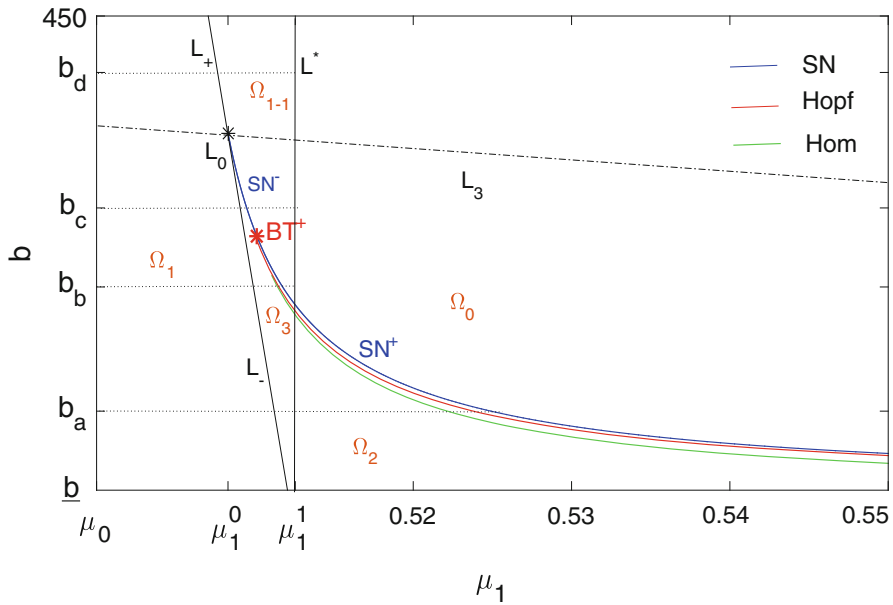
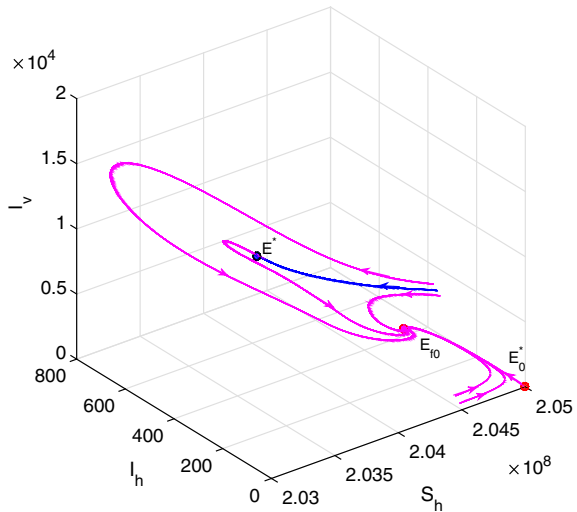


**Fig. 5** Bifurcation curves in  $(\mu_1, b)$  plane (Color figure online)

**Fig. 6** The phase portrait of (4) at  $BT^+(\mu_1, b) = (\mu_1^0, b^0)$ .  $E^*$  is the Bogdanov–Takens point of order 2. System (4) has a stable equilibrium  $E_{f0}$  and an unstable DFE  $E_0^*$



defined by  $R_c^* = 1 + \gamma$  in  $(\mu_1, b)$  plane, where  $b_2$  is defined by Eq. (24). Curve  $L_3$ :  $b = b_3(\mu_1)$ , where  $b_3$  is defined by (26). Denote intersection point of curve  $L$  and  $L_3$  be  $L_0 = (\mu_1^0, b_0)$ .  $L_0$  divides  $L$  into two parts  $L_+$  ( $b > b_0$ ) and  $L_-$  ( $b < b_0$ ). System (4) has a backward bifurcation with endemic equilibrium on the line  $L_-$ . In addition, saddle-node bifurcation curve  $SN$  also satisfies  $b = b_1(\mu_1)$ , where  $b = b_1(\mu_1)$  satisfies  $\Delta_D(b_1) = 0$ .

We define

$$\begin{aligned}\Omega_1 &= \{ (\mu_1, b) \mid b < b_2(\mu_1), \mu_1 > \mu_0 \}, \\ \Omega_{1-1} &= \{ (\mu_1, b) \mid b > \max\{b_1(\mu_1), b_2(\mu_1)\}, \mu_0 < \mu_1 < \mu_1^1 \}, \\ \Omega_3 &= \{ (\mu_1, b) \mid b_2(\mu_1) < b < \min\{\bar{b}(\mu_1), b_1(\mu_1), b_3(\mu_1)\}, \mu_1^0 < \mu_1 < \mu_1^1 \}, \\ \Omega_2 &= \{ (\mu_1, b) \mid b < \min\{\bar{b}(\mu_1), b_1(\mu_1), b_3(\mu_1)\}, \mu_1 > \mu_1^1 \}, \\ \Omega_0 &= \{ (\mu_1, b) \mid b > b_1(\mu_1), \mu_1 > \mu_1^1 \}.\end{aligned}$$

Based on the above discussion, system (4) has 0, 1, 1, 2 and 3 positive equilibria in regions  $\Omega_0, \Omega_1, \Omega_{1-1}, \Omega_2$  and  $\Omega_3$ , respectively.

## 5.2 Bifurcation Diagram in $(R_c^*, I_h)$ Plane

As  $R_c^*$  is biologically significant, it is necessary to plot the bifurcation diagram on  $(R_c^*, I_h)$  plane. As  $R_c^*$  is a monotone decreasing function of  $\mu_1$ , we change  $\mu_1$  with different  $b$ . Choose four representative values of  $b = b_a, b_b, b_c, b_d$  displayed in Fig. 5, to illustrate the all possible bifurcation diagrams in  $(R_c^*, I_h)$  plane.

For  $b = b_a = 100$ ,  $\mu_1$  or  $R_c^*$  changes, in turn, from region  $\Omega_0, \Omega_2, \Omega_3$  to  $\Omega_1$  shown in Fig. 5. A typical bifurcation diagram is illustrated in Fig. 7a. The bifurcation from the DFE at  $R_c^* = 1$  is forward, and the bifurcation from an endemic equilibrium at  $R_c^* = 1 + \gamma$  is backward. This bifurcation phenomenon gives rise to the existence of multiple endemic equilibria. We can see from Fig. 7a that the disease does not die out when  $R_c^* < 1$ . This is a very important conclusion for disease control. Biologically, for  $R_c^* < 1$ , if available medical resources are not enough, and at the beginning of endemic, by the introduction of enough new cases (due to the sudden influx of infectious individuals), then force epidemic outbreaks that could stabilize at an endemic state. If few patients were introduced, then the disease may be eradicated. Thus, control measures that focus on reducing  $R_c^*$  so that  $R_c^* < 1$  may not be successful in eradicating the disease unless  $R_c^*$  is lowered a secondary threshold value  $R_c^{*c}$ .

If we increase  $b$  so that  $1 < R_c^{*c} < 1 + \gamma$ , there is no endemic equilibrium when  $R_c^* < 1$ . In this case, choosing  $b = b_b = 210$  and  $b = b_c = 280$ , backward bifurcation diagrams in  $(R_c^*, I_h)$  are shown in Fig. 7b, c, respectively. Backward bifurcation and saddle-node bifurcation occur in cases shown in Fig. 7a–c. One unstable limit cycle bifurcated from subcritical Hopf bifurcation disappears from homoclinic bifurcation in cases shown in Fig. 7a, b. If  $b$  is so large that  $b > b_0$  (Fig. 5), choosing  $b = b_d = 400$ , then system (4) does not have a backward bifurcation, and only forward bifurcation is illustrated in Fig. 7d, where the bifurcation at  $R_c^* = 1$  is forward and system (4) has a stable unique endemic equilibrium for all  $R_c^* > 1$ . Figure 7 suggests that an insufficient capacity of available medical resources  $b$  is a key factor of the backward bifurcation. The dashed curve indicates the unstable equilibrium, and the solid curve represents the stable equilibrium in next all bifurcation diagrams.

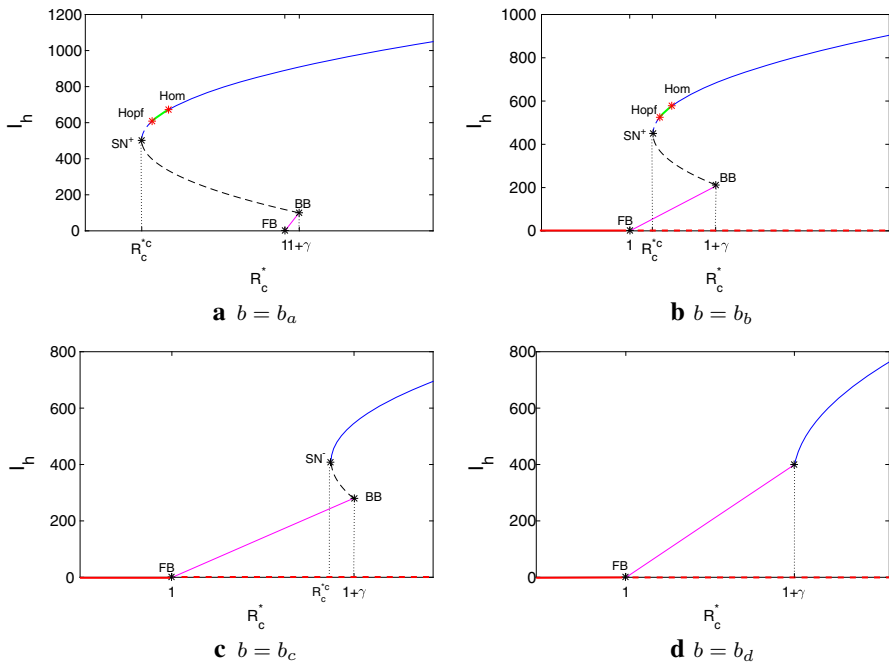


**Fig. 7** Bifurcation diagrams in  $(R_c^*, I_h)$  plane of system (4) with different  $b$ . FB represents forward bifurcation and BB represents backward bifurcation

### 5.3 Bifurcation Diagram in $(b, I_h)$ Plane

Now, fix  $\mu_1$  and continuously change  $b$  for Fig. 5. Choosing  $\mu_1 = 0.52$ , we calculate  $R_c^* = 0.9905 < 1$ . A bifurcation diagram in  $(b, I_h)$  plane is displayed in Fig. 8a. System (4) presents complicated dynamic when  $b < b_1 = 120.5$ , and these rich dynamics finally disappear through the saddle-node bifurcation when  $b = b_1$ . From  $b = b_1$ , as  $b$  decreases, the unstable limit cycle bifurcated from subcritical Hopf bifurcation disappears from homoclinic bifurcation. Figure 8a indicates there exist two endemic equilibria when  $b < b_1$ ; otherwise, there is no endemic equilibrium. Figure 8b shows that there always exists endemic equilibrium for  $R_c^* > 1$ . So increasing the capacity of available medical resources can only reduce limited number of the infectious, but cannot eliminate the disease as shown in Fig. 8b. Next, we will discuss the effect of available medical resources  $b$  on the dynamical behavior of system (4) for  $R_c^* < 1$ .

### 5.4 Stability of System (4)

Consider system (4) with the parameter  $\mu_1 = 0.52$  for Fig. 5, the corresponding value  $R_c^*$  is 0.9905. We change the value of  $b$  and fix other parameters unchanged and illustrate the effect of available medical resources  $b$  on the dynamical behavior of system (4).



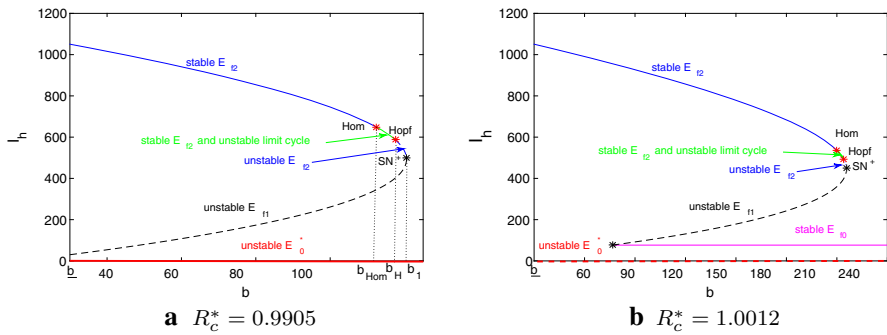


**Fig. 8** Bifurcation diagrams in  $(b, I_h)$  plane of system (4) for **a**  $R_c^* = 0.9905 < 1$  with  $\mu_1 = 0.52$ , and **b**  $R_c^* = 1.0012 > 1$  with  $\mu_1 = 0.5115$

For  $R_c^* = 0.9905 < 1$  (i.e.,  $\mu_1 = 0.52$ ), Fig. 9 displays the six types of dynamical behaviors of system (4) shown in Fig. 8a. When  $b = 125 > b_1$ , system (4) has a unique stable DFE  $E_0^*$  and has no endemic equilibrium (Fig. 9a). As  $b$  decreases, when  $b$  crosses  $b_1$ , system (4) undergoes a saddle-node bifurcation (Fig. 9b); there are two endemic equilibria: a saddle  $E_{f1}$  and an unstable node  $E_{f2}$ . Then, the node changes into a focus (Fig. 9c). As  $b$  decreases,  $E_{f2}$  changes stability and an unstable limit cycle marked black curve around the stable equilibrium  $E_{f2}$  is bifurcated from subcritical Hopf bifurcation (Fig. 9d). When  $b = b_{\text{Hom}}$  ( $b_{\text{Hom}} = 112.5$ ), the limit cycle disappears from homoclinic bifurcation, and system (4) has a homoclinic orbit marked green curve to the saddle (Fig. 9e). Then, for  $b = 100 < b_{\text{Hom}}$ , bistability occurs. That is, a stable DFE coexists with a stable endemic equilibrium shown in Fig. 9f.

Biologically, this conclusion shows that the epidemic levels with limited medical resources are sensitive to parameters and initial conditions. When the medical resources is sufficient (i.e.,  $b > b_1$ ), the disease can be eliminated (Fig. 9a). When the medical resources are below threshold (i.e.,  $b < b_1$ ), saddle-node bifurcation occurs (Fig. 9b). In this case, there are rich behaviors for the epidemic levels, such as multiple stable or epidemic break out in periodic manner. The occurrence of periodic phenomena is due to branching Hopf bifurcation. Therefore, the recurrence of the Zika disease is possible when the initial number of infected individuals is in some certain ranges (Fig. 9d). As the medical resources decrease, the emergence of homoclinic bifurcation breaks this periodic phenomena and makes the epidemic levels bistable (Fig. 9e, f). In this case, whether Zika disease dies out or outbreak depending on initial number of infected individuals. Hence, biologically our results have important consequences for the control of Zika disease.

## 5.5 The Comparison of System (4) and System (5)

Fixing  $\mu_1 = 0.52$ ,  $b = 100$  and other parameters in Table 2, continuously vary  $\beta_1$ . Figure 10 shows bifurcation curves from  $I_h$  versus  $\beta_1$  for system (4) (black curves) and system (5) (red curves). By comparing black and red curves in Fig. 10, it is

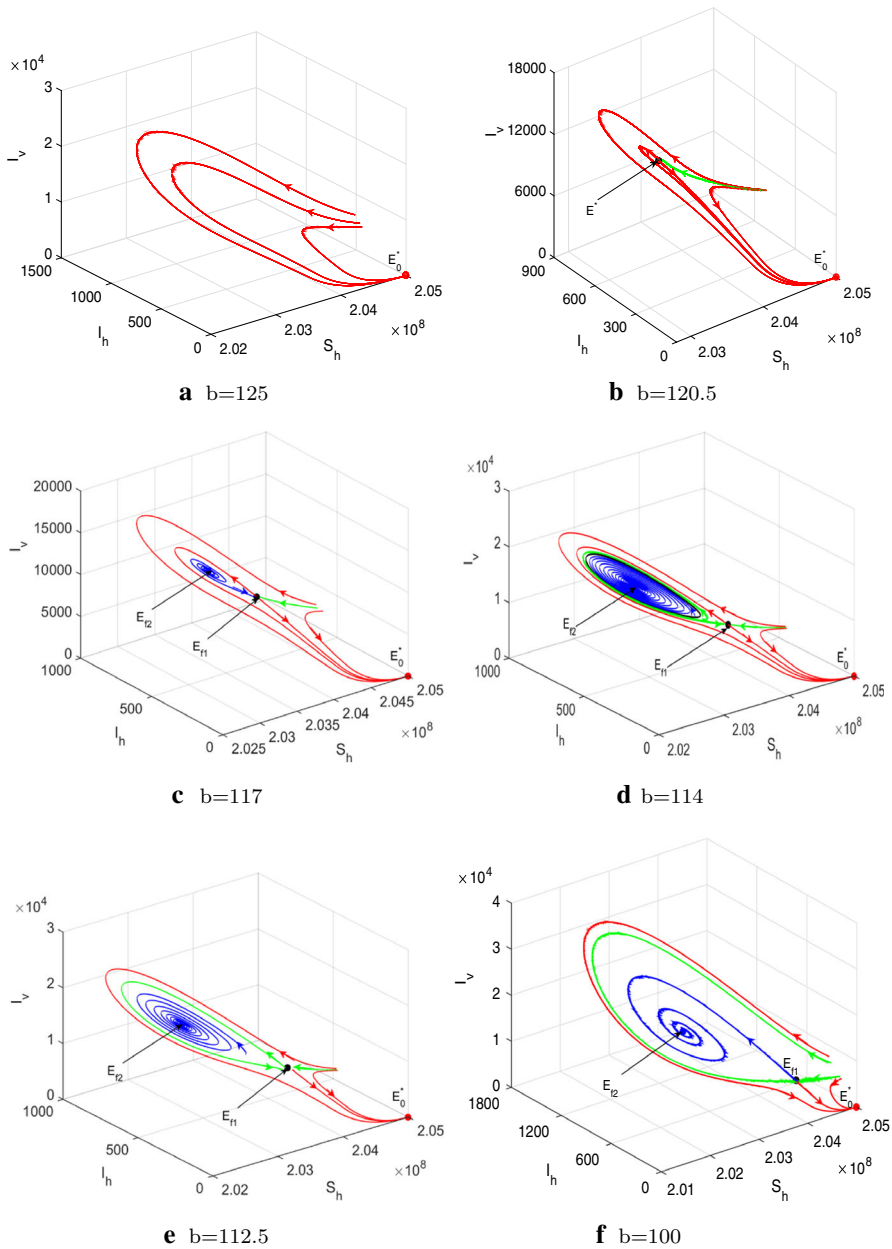


**Fig. 9** The phase diagram of system (4) for  $R_c^* = 0.9905 < 1$ . **a** System (4) has a stable DFE  $E_0^*$ . **b** An unstable node  $E_{f2}$  and a saddle  $E_{f1}$  of system (4) coalesce at the equilibrium  $E^*$ .  $E_0^*$  is locally stable. **c** System (4) has an unstable equilibrium  $E_{f2}$ , a stable DFE  $E_0^*$  and a saddle  $E_{f1}$ . **d** System (4) has an unstable limit cycle marked black curve near the locally stable equilibrium  $E_{f2}$ .  $E_0^*$  and  $E_{f2}$  are locally stable.  $E_{f1}$  is a saddle. **e** System (4) has a homoclinic orbit marked green curve to the saddle  $E_{f1}$ .  $E_0^*$  and  $E_{f2}$  are locally stable. **f** System (4) has two locally stable equilibria: a DFE  $E_0^*$  and an endemic equilibrium  $E_{f2}$ . The other endemic equilibrium  $E_{f1}$  is a saddle (Color figure online)

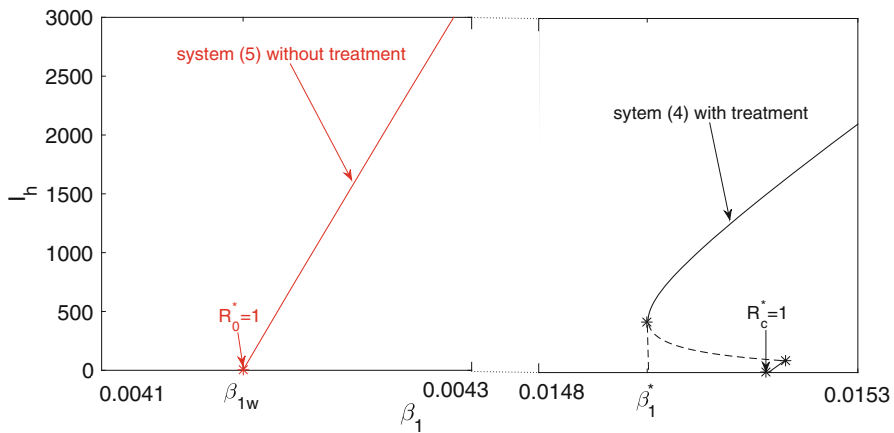


**Fig. 10** Bifurcation curves from  $I_h$  versus  $\beta_1$  for system (4) (black curves) and system (5) (red curves) (Color figure online)

found that system (4) and system (5) have completely different dynamical behaviors. When  $\beta_{1w} < \beta_1 < \beta_1^*$ , for system (4) with treatment, the disease-free equilibrium is the unique and stable state, while for system (5) without treatment, disease-free equilibrium is unstable and endemic equilibrium is globally asymptotically stable. Biologically, without treatment will overestimate the emergence of Zika epidemic and increase the risk of Zika outbreak. So, the non-smooth treatment recovery rate plays an important role in generating complex dynamics.

## 6 A Numerical Application to Brazil

### 6.1 Parameters Estimation and Reproduction Number

We collect weekly reported accumulated cases that start from thirteenth week of 2016 and use the weekly cases from March 25, 2016, to April 14, 2018, from the Brazil Ministry of Health (<http://portalms.saude.gov.br/boletins-epidemiologicos>) and the World Health Organization ([http://www.paho.org/hq/index.php?option=com\\_content&view=article&id=11117](http://www.paho.org/hq/index.php?option=com_content&view=article&id=11117)). So, we choose the thirteenth week in 2016 as the starting date of the initial observation and corresponding reported accumulated case as the initial value. We apply system (4) to fit the accumulated cases (due to lack of information about weekly new cases, here, we only use our model to fit the accumulated cases) in Brazil and take a week as the unit time. So the period is about 106 weeks in our study. Some parameters values can be obtained from previous literatures and Web sites about Zika for Brazil, but some parameters values are unknown due to lack of information about Zika. Based on the ideas in Sasmal et al. (2018), we let  $N_v = c_1 \times N_h$  and  $I_v(0) = c_2 \times N_h$ . In addition, the initial values  $S_h(0)$  and  $I_h(0)$  cannot be obtained directly, So, the values of  $c_1$ ,  $c_2$ ,  $S_h(0)$  and  $I_h(0)$  can be estimated

**Table 3** Parameter descriptions

Parameter	Range	Value	References
$a$	(2.1, 7)	2.1	Andraud et al. (2011)
$\beta_1$	(0, 0.97)	0.12	Zhang (2017)
$\beta_2$	(0, 0.97)	0.225	Zhang (2017)
$\beta_3$	(0.001, 0.28)	0.1	Sasmal et al. (2018)
$\mu_0$		1.17	Estimation
$\mu_1$		1.5	Estimation
$r$	$\left(\frac{7}{30}, \frac{7}{2}\right)$	0.5	Gourinat et al. (2015)
$N_h$		$2.05 \times 10^8$	<a href="http://population.city/brazil/#cities">http://population.city/brazil/#cities</a>
$d_h$		$\frac{1}{75 \times 52}$	Wiratsudakul et al. (2018)
$d_v$	$\left(\frac{7}{50}, \frac{7}{4}\right)$	0.3	Andraud et al. (2011)
$b$		5000	Assumption
$\underline{b}$		2000	Assumption
$c_1$		3.7	Estimation
$c_2$		0.00033	Estimation
$S_h(0)$		$1.540 \times 10^8$	Estimation
$I_h(0)$		$1.845 \times 10^4$	Estimation

as parameters by using least-square estimation method. Denote unknown parameters as  $\Theta = (\mu_0, \mu_1, c_1, c_2, S_h(0), I_h(0))$ .

Let  $y(t)$  be theoretic accumulated cases, and its change with time is described as  $\frac{dy(t)}{dt} = a\beta_1 \frac{I_v S_h}{N_h} + \beta_3 \frac{I_h S_h}{N_h}$ , where  $S_h, I_h, I_v$  satisfies system (4), and  $\bar{y}(t)$  is surveillance data in week  $t$ , with  $y(0) = \bar{y}(0)$ . Next, the least-square estimation method is used to calculate the parameters values to minimize the objective function

$$J = \frac{1}{n} \sum_{t=0}^{n-1} (y(t) - \bar{y}(t))^2,$$

in which  $n$  is the number of reported data.

By applying the real data and system (4), the vector of parameters  $\Theta$  is estimated in Table 3.

Through some rational assumptions and parameter estimation, the good fitting result for the accumulated cases is given in Fig. 11. We can see that the slope of the fitting cure increases gradually, which means that Zika is still deteriorating in the early stages of the epidemic. Later on, the slope of accumulated cases gradually tends to the level. We estimate the control reproduction number  $R_c = 0.8822$ , where the term of  $R_c$  concerning the mosquito transmission is  $R_{hv} = 0.8568$ , and the sexual transmission is  $R_{hh} = 0.05$ . Further, by substituting parameters values shown in Table 3 into the expression (10) of  $\hat{R}_c^*$ , one obtains  $\hat{R}_c^* = 0.9410 < 1$ . From Theorem 5, the DFE  $E_0^*$

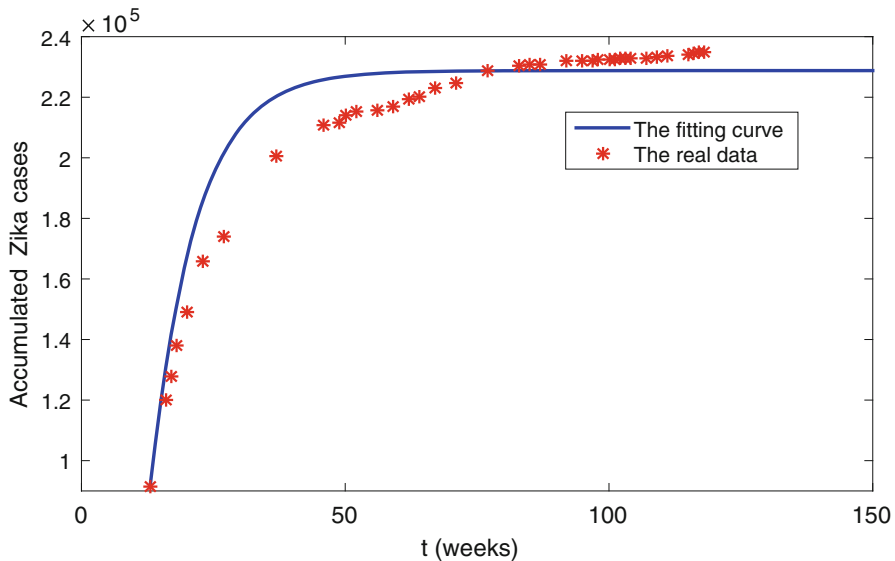


**Fig. 11** Fitting curve of real data from March 25, 2016, to April 14, 2018, and prediction result for the following 30 weeks by deterministic system (4), where the red star denotes the real data of accumulated Zika cases (Color figure online)

of system (4) is the unique equilibrium and globally stable. This means that in Brazil, Zika epidemic will eventually disappear.

If effective measures are not taken, then the basic reproduction number  $R_0$ , an indicator of the initial transmissibility of the Zika disease, is estimated to be 1.8162, concerning the mosquito transmission is  $R_{hvw} = 1.7133$ , and the sexual transmission is  $R_{hhw} = 0.1999$ . From Theorem 2, endemic equilibrium  $E_w^*$  of system (5) is globally asymptotically stable. It means that without any effective measures, Zika epidemic erupts in Brazil.

## 6.2 The Effect of Parameters $b$ , $\mu_1$ , $\beta_1$ and $\beta_3$ on the Final Accumulated Cases of Zika in Brazil

**The effect of limited medical resources  $b$**  From Fig. 12a, we can show that the more capacity of available medical resources is, the smaller the final size of accumulated cases will be. If capacity of available medical resources can only treat 3000 infected people per week, the final size of accumulated Zika in Brazil will reach 241,900 cases which is 6900 more than that of real reported data. If capacity of available medical resources is so much that 10,000 infected people enough can be treated per week, the final size of accumulated Zika cases will reduce 11,500 cases.

**The effect of maximum treatment recovery rate  $\mu_1$**  It can also greatly reduce the magnitude of the final accumulated cases by increasing the maximum treatment rate from Fig. 12b. If the maximum treatment rate is equal to that of minimum (i.e.,  $\mu_1 = \mu_0$ ), the final size of accumulated Zika in Brazil will reach 282,100 cases which

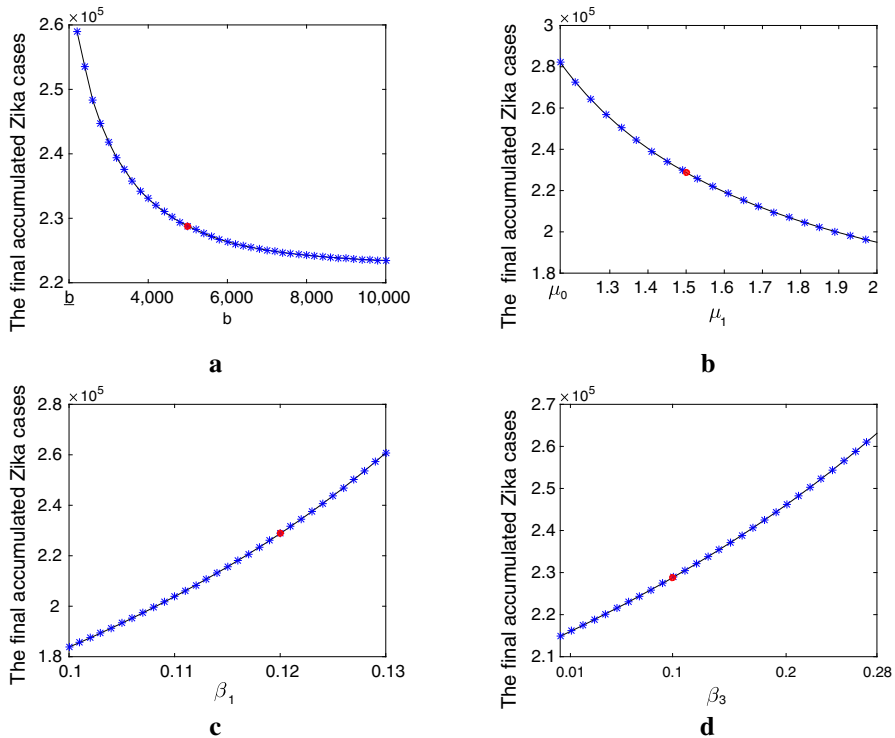


**Fig. 12** The final accumulated cases of Zika in Brazil with respect to  $b$ ,  $\mu_1$ ,  $\beta_1$  and  $\beta_3$ . The red point corresponds to **a**  $b = 5000$ , **b**  $\mu_1 = 1.5$ , **c**  $\beta_1 = 0.12$  and **d**  $\beta_3 = 0.1$ , respectively. All other parameters values are shown in Table 3 (Color figure online)

is 47,100 more than that of real reported data. If the maximum treatment rate is 2 per week, that is, the infected people can recover in 3.5 days, the final size of accumulated Zika cases will be 41,000 less than that of real reported data.

**The effect of transmission probability from mosquito to human  $\beta_1$  and sexual transmission rate  $\beta_3$**  Figure 12c, d shows the effect of two critical parameters in spread of Zika: transmission probability from mosquitoes to humans  $\beta_1$  and sexual transmission rate  $\beta_3$  on the final size of accumulated Zika. From Fig. 12c, d, the final scale of Zika outbreaks in Brazil will get larger when the  $\beta_1$  (or  $\beta_3$ ) increases which is consistent with the actual situation. From Fig. 12, we obtain that increasing the capacity of available medical resources, improving the maximum treatment efficiency, eradicating mosquitoes and protecting oneself from infection during intercourse are effective methods to decrease the final size of accumulated Zika case in Brazil.

The effect of the capacity of available medical resources on the final accumulated cases of Zika is discussed above. Next, we consider the relationship between the mean duration from infected to recovered individuals  $\mu^{-1}$  [ $\mu$  defined by (1)] and available medical resources.

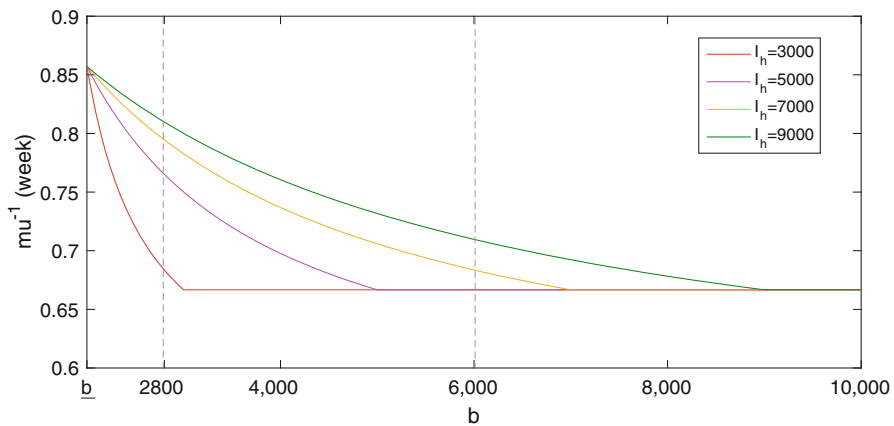


**Fig. 13** The mean duration from infected to recovered individuals  $\mu^{-1}$  with respect to  $b$ . Other parameters values are shown in Table 3

### 6.3 The Effect of Parameter $b$ on the Mean Duration from Infected to Recovered Individuals $\mu^{-1}$

In this subsection, we will present a relation between  $b$  and  $\mu^{-1}$ . Choose  $I_h = 3000, 5000, 7000, 9000$ , respectively. It follows from Fig. 13 that the mean duration from infected to recovered individuals is decreasing as capacity of available medical resources increases when available medical resources are not sufficient (i.e.,  $b < I_h$ ) and keeps the shortest time when the capacity of available medical resources for treatment is sufficient (i.e.,  $b > I_h$ ). From Fig. 13, if keep  $b = 2800$  unchanged, then  $\mu^{-1}$  will get smaller when infectious humans decrease. The mean time of infected to recovered individuals is 0.8095 week for 9000 infectious cases, but 0.6826 week for 3000 infectious cases. If choose  $b = 6000$ , then the mean time of infected to recovered individuals is all 0.6667 week for 3000 and 5000 infectious cases. From Fig. 13, we obtain that increasing the capacity of available medical resources can effectively shorten sick time.

## 7 Discussion

In this paper, we build a model which incorporates both mosquito-borne and sexual transmission routes with a non-smooth treatment recovery rate to describe the effect of available medical resources. Our system extends the previous Zika models (Funk 2016; Kucharski 2016; Gao 2016; Wang et al. 2017; Agosto et al. 2017a,b,a; Pizza 2016; Shah et al. 2017; Zhang 2017; Tang et al. 2016) in which dynamics of the systems completely depend on the basic reproduction number. In contrast to their work and to classic epidemic systems, our finds reveal that  $R_c$  is not enough to determine the dynamical behaviors, and the non-smooth treatment recovery rate plays an important role in generating complex dynamics. We prove that the model with LMRs undergoes backward bifurcation, Hopf bifurcation and Bogdanov–Takens bifurcation of codi-

mension 2. Biologically, these rich dynamics show that trends of Zika epidemic may be extinction, multiple stable or epidemic breakout in periodic pattern. It shows that the model with limited medical resources is sensitive to parameters and initial conditions.

Our system can undergo a forward bifurcation at DFE, and a backward bifurcation at endemic equilibrium due to LMRs (Fig. 7a). Different from previous models (Abdelrazec et al. 2016; Shan and Zhu 2014; Imran et al. 2017), the backward bifurcation occurs at DFE. We find that stable DFE may coexist with two endemic equilibria when the control reproduction number is less than unity. Moreover, bistable endemic equilibria may coexist when the control reproduction number is more than unity. From Fig. 7b, in case  $R_c^{*c} \geq 1$ , although system (4) has a backward bifurcation with endemic equilibrium, the disease also can be eradicated when  $R_c^* < 1$ . In case  $R_c^{*c} < 1$ , the disease cannot be eradicated simply by reducing  $R_c^*$  below 1 unless  $R_c^*$  falls below a secondary threshold  $R_c^{*c}$  or  $b > b_1(\mu_1)$ .

The capacity of available medical resources does not change the control reproduction number in our model; this is in agreement with Wang (2006) and Shan and Zhu (2014). However, the capacity of available medical resources could be used to control the transmission of Zika when  $R_c^* < 1$  illustrated in Fig. 8a. We also find a threshold value  $b_1$ . When  $R_c^* < 1$ , there exist two endemic equilibria when  $b \leq b_1$ , and otherwise, no endemic equilibria are shown in Fig. 8a. Our analysis suggests that backward bifurcation is generated by changing  $b$  for  $R_c^* < 1$ . For the control strategy, we can wipe out the disease by increasing available medical resources. For  $R_c^* > 1$ , increasing  $b$  can reduce only a limited number of the infectious; it cannot eliminate the Zika disease shown in Fig. 8b.

In our model, if we do not consider the available medical resources, then the treatment recovery rate is 0. In this case, model (5) without treatment does not undergo backward bifurcations. By comparison with model (4), without treatment will overestimate the emergence of Zika epidemic and increase the risk of Zika outbreak (Fig. 10). So, the non-smooth treatment recovery rate plays an important role in generating complex dynamics.

As an application, we apply the model to estimate the accumulated cases in Brazil from March 25, 2016, to April 14, 2018, and get reasonable matches. We estimate the control reproduction number  $R_c = 0.8822$ , where the term of  $R_c$  concerning the mosquito transmission is  $R_{hv} = 0.8568$  and the sexual transmission is  $R_{hh} = 0.05$ . This means that in Brazil, two transmission routes play more important roles in the transmission of Zika virus. From Theorem 5, Zika epidemic in Brazil will eventually disappear. Through simulation analysis,  $b$  and  $\mu_1$  are very key parameters. From Fig. 12, it is obvious that accumulated case is decreasing as  $b$  (or  $\mu_1$ ) increases which is consistent with the actual situation. It is a rather challenging work to find the minimum capacity of available medical resources for the control of Zika transmission in Brazil. In future work, we will determine an optimal value for the capacity of available medical resources.

To establish a tractable system to model the mosquito–human interactions, this work considers only a simplified life cycle of mosquitoes. In fact, the mosquito has a complex life-cycle. Climate factors play a crucial role in MBDs and can influence various aspects of the life cycle of mosquito, including mating, reproduction, biting behavior and mortality. The spatial spread of Zika virus actually exists because of



the movement of humans and the different distributions of different geographic *Aedes* mosquitoes. Because of the limited information and data, we do not consider spatial spread. It will be interesting to study the effect of climate changes, human movements and distributions of *Aedes* mosquitoes on the transmission of Zika in our system. We leave these for future investigation.

**Acknowledgements** We are very grateful to anonymous referees and editor for careful reading and helpful suggestions which led to an improvement of our original manuscript. The work is partially supported by the National Natural Science Foundation of China (Nos. 11571170, 11971013) and funding of Jiangsu Innovation Program for Graduate Education KYZZ16\_0162 and CIHR and NSERC of Canada.

## Appendix A: Proof of Theorem 1

**Proof** Consider the Lyapunov function

$$V_w = \left( \frac{S_h}{S_{hw}^0} - \ln \frac{S_h}{S_{hw}^0} - 1 \right) + \frac{I_h}{N_h} + \frac{(r + d_h)(1 - R_{hhw})}{a\beta_2} \cdot \frac{I_v}{N_v}$$

in  $\Gamma$ . if  $R_0^* < 1$ , then  $R_{hhw} < 1$ . One has  $V_w \geq 0$ , and  $V_w = 0$  if only if  $S_h = S_{hw}^0$ ,  $I_h = 0$ ,  $I_v = 0$ . So,  $V_w$  is a positive definite function. The orbital derivative of  $V_w$  along the solution of system (5) can be written as

$$\begin{aligned} \frac{dV_w}{dt} \Big|_{(5)} &= \frac{1}{S_h S_{hw}^0} \left( S_h - S_{hw}^0 \right) \frac{dS_h}{dt} + \frac{1}{N_h} \frac{dI_h}{dt} + \frac{(r + d_h - \beta_3)}{a\beta_2 N_v} \frac{dI_v}{dt} \\ &= \frac{1}{S_h S_{hw}^0} (S_h - S_{hw}^0) \left( \Lambda_h - \frac{a\beta_1 S_h I_v}{N_h} - \beta_3 \frac{I_h S_h}{N_h} - d_h S_h \right) \\ &\quad + \frac{1}{N_h} \left( \frac{a\beta_1 S_h I_v}{N_h} + \beta_3 \frac{I_h S_h}{N_h} - (r + d_h) I_h \right) \\ &\quad + \frac{(r + d_h - \beta_3)}{a\beta_2 N_v} \left( a\beta_2 \frac{I_h (N_v - I_v)}{N_h} - d_v I_v \right) \\ &= - \frac{d_h}{S_h S_{hw}^0} (S_{hw}^0 - S_h)^2 - (1 - R_{hhw}) \frac{(r + d_h)}{N_v N_h} I_v I_h \\ &\quad - (1 - R_{0w}^*) \frac{d_v (r + d_h)}{a\beta_2 N_v} I_v. \end{aligned}$$

If  $R_0^* < 1$ , then  $\frac{dV_w}{dt} \Big|_{(5)} \leq 0$ . So,  $E_{0w}$  is stable. It is easy to see that  $E_{0w}$  is the largest positively invariant set contained in  $\frac{dV_w}{dt} \Big|_{(5)} = 0$ . Thus, from the LaSalle theorem,  $E_{0w}$  is globally attractive. Thus,  $E_{0w}$  is globally stable if  $R_0^* < 1$ .  $\square$

## Appendix B: Proof of Theorem 2

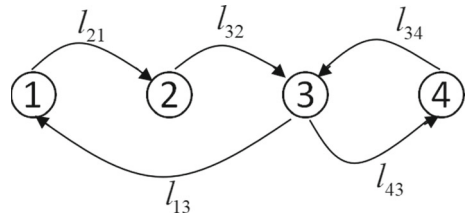
**Proof** If  $R_0^* > 1$ , then system (5) has a unique endemic equilibrium  $E_w^*$ . Let

$$\begin{aligned} V_i &= S_{hw}^* \left( \frac{S_h}{S_{hw}^*} - \ln \left( \frac{S_h}{S_{hw}^*} \right) - 1 \right), i = 1, 2, \\ V_3 &= I_{hw}^* \left( \frac{I_h}{I_{hw}^*} - \ln \left( \frac{I_h}{I_{hw}^*} \right) - 1 \right), \\ V_4 &= I_{vw}^* \left( \frac{I_v}{I_{vw}^*} - \ln \left( \frac{I_v}{I_{vw}^*} \right) - 1 \right). \end{aligned} \quad (38)$$

Differentiate  $V_i$  along the solution of system (5). One has

$$\begin{aligned} \left. \frac{dV_i}{dt} \right|_{(5)} &= \left( 1 - \frac{S_{hw}^*}{S_h} \right) \left( \Lambda_h - a\beta_1 \frac{I_v S_h}{N_h} - \beta_3 \frac{I_h S_h}{N_h} - d_h S_h \right) \\ &= \left( 1 - \frac{S_{hw}^*}{S_h} \right) \left( \frac{a\beta_1}{N_h} (I_{vw}^* S_{hw}^* - I_v S_h) + \frac{\beta_3}{N_h} (I_{hw}^* S_{hw}^* - I_h S_h) \right. \\ &\quad \left. + d_h (S_{hw}^* - S_h) \right) \\ &= -\frac{d_h}{S_h} (S_h - S_{hw}^*)^2 + \frac{a\beta_1 I_{vw}^* S_{hw}^*}{N_h} \left( 1 - \frac{S_{hw}^*}{S_h} - \frac{I_v S_h}{I_{vw}^* S_{hw}^*} + \frac{I_v}{I_{vw}^*} \right) \\ &\quad + \frac{\beta_3 I_{hw}^* S_{hw}^*}{N_h} \left( 1 - \frac{S_{hw}^*}{S_h} - \frac{I_h S_h}{I_{hw}^* S_{hw}^*} + \frac{I_h}{I_{hw}^*} \right) \\ &\leq \frac{a\beta_1 I_{vw}^* S_{hw}^*}{N_h} \left( \frac{I_v}{I_{vw}^*} - \ln \left( \frac{I_v}{I_{vw}^*} \right) - \frac{I_v S_h}{I_{vw}^* S_{hw}^*} + \ln \left( \frac{I_v S_h}{I_{vw}^* S_{hw}^*} \right) \right) \\ &\quad + \frac{\beta_3 I_{hw}^* S_{hw}^*}{N_h} \left( \frac{I_h}{I_{hw}^*} - \ln \left( \frac{I_h}{I_{hw}^*} \right) - \frac{I_h S_h}{I_{hw}^* S_{hw}^*} + \ln \left( \frac{I_h S_h}{I_{hw}^* S_{hw}^*} \right) \right), \\ &\triangleq l_{21} G_{21} + l_{43} G_{43}, i = 1, 2, \\ \left. \frac{dV_3}{dt} \right|_{(5)} &= \left( 1 - \frac{I_{hw}^*}{I_h} \right) \left( a\beta_1 \frac{I_v S_h}{N_h} + \beta_3 \frac{I_h S_h}{N_h} - r I_h - d_h I_h \right) \\ &= \left( 1 - \frac{I_{hw}^*}{I_h} \right) \left( \frac{a\beta_1}{N_h} \left( I_v S_h - \frac{I_{vw}^* S_{hw}^* I_h}{I_{hw}^*} \right) + \frac{\beta_3}{N_h} (I_h S_h - I_h S_{hw}^*) \right) \\ &\leq \frac{a\beta_1 I_{vw}^* S_{hw}^*}{N_h} \left( \frac{I_v S_h}{I_{vw}^* S_{hw}^*} - \ln \left( \frac{I_v S_h}{I_{vw}^* S_{hw}^*} \right) - \frac{I_h}{I_{hw}^*} + \ln \left( \frac{I_h}{I_{hw}^*} \right) \right) \\ &\quad + \frac{\beta_3 I_{hw}^* S_{hw}^*}{N_h} \left( \frac{I_h S_h}{I_{hw}^* S_{hw}^*} - \ln \left( \frac{I_h S_h}{I_{hw}^* S_{hw}^*} \right) - \frac{I_h}{I_{hw}^*} + \ln \left( \frac{I_h}{I_{hw}^*} \right) \right) \end{aligned}$$

**Fig. 14** The weighted digraph  $(\mathcal{G}, M)$



$$\begin{aligned}
 &\triangleq l_{32}G_{32} + l_{34}G_{34}, \\
 \frac{dV_4}{dt} \Big|_{(5)} &= \left(1 - \frac{I_{vw}^*}{I_v}\right) \left(a\beta_2 \frac{I_h(N_v - I_v)}{N_h} - d_v I_v\right) \\
 &\leq \frac{a\beta_2 N_v}{N_h} I_{hw}^* \left(\frac{I_h}{I_{hw}^*} - \ln\left(\frac{I_h}{I_{hw}^*}\right) - \frac{I_v}{I_{vw}^*} + \ln\left(\frac{I_v}{I_{vw}^*}\right)\right) \\
 &\triangleq l_{13}G_{13}.
 \end{aligned}$$

Here,  $l_{21} = l_{32} = \frac{a\beta_1 I_{vw}^* S_{hw}^*}{N_h}$ ,  $l_{34} = l_{43} = \frac{\beta_3 I_{hw}^* S_{hw}^*}{N_h}$ ,  $l_{13} = \frac{a\beta_2 N_v}{N_h} I_{hw}^*$ ,  $G_{21} = \frac{I_v}{I_{vw}^*} - \ln\left(\frac{I_v}{I_{vw}^*}\right) - \frac{I_v S_h}{I_{vw}^* S_{hw}^*} + \ln\left(\frac{I_v S_h}{I_{vw}^* S_{hw}^*}\right)$ ,  $G_{43} = \frac{I_h}{I_{hw}^*} - \ln\left(\frac{I_h}{I_{hw}^*}\right) - \frac{I_h S_h}{I_{hw}^* S_{hw}^*} + \ln\left(\frac{I_h S_h}{I_{hw}^* S_{hw}^*}\right)$ ,  $G_{32} = \frac{I_v S_h}{I_{vw}^* S_{hw}^*} - \ln\left(\frac{I_v S_h}{I_{vw}^* S_{hw}^*}\right) - \frac{I_h}{I_{hw}^*} + \ln\left(\frac{I_h}{I_{hw}^*}\right)$ ,  $G_{34} = \frac{I_h S_h}{I_{hw}^* S_{hw}^*} - \ln\left(\frac{I_h S_h}{I_{hw}^* S_{hw}^*}\right) - \frac{I_h}{I_{hw}^*} + \ln\left(\frac{I_h}{I_{hw}^*}\right)$ ,  $G_{13} = \frac{I_h}{I_{hw}^*} - \ln\left(\frac{I_h}{I_{hw}^*}\right) - \frac{I_v}{I_{vw}^*} + \ln\left(\frac{I_v}{I_{vw}^*}\right)$ .

Now, denote a weight matrix  $M = (a_{ij})_{4 \times 4}$  and the corresponding weighted digraph  $(\mathcal{G}, M)$  is shown in Fig. 14. Denote  $s(\mathcal{C})$  be the arc set of  $\mathcal{C}$ . Then, for each cycle  $\mathcal{C}$ , one has  $\sum_{(i,j) \in s(\mathcal{C})} G_{ij} = 0$ . Thus, from Theorem 3.5 in Shuai and Van den Driessche (2013), there exist  $\bar{c}_i \geq 0$ ,  $i = 1, 2, \dots, 4$ , such that  $V = \sum_{i=1}^4 \bar{c}_i V_i$  is a Lyapunov function of system (5) and  $\frac{dV}{dt} \Big|_{(5)} \leq 0$ . Using the same step in Wang and Zhao (2019),  $V = \sum_{i=1}^4 \bar{c}_i V_i$  is a positive definite function. So,  $E_w^*$  is stable.  $E_w^*$  is the largest positively invariant set contained in  $\frac{dV}{dt} \Big|_{(5)} = 0$ . Thus, from the LaSalle theorem,  $E_w^*$  is globally attractive. Thus,  $E_w^*$  is globally stable in the region  $\Gamma \setminus E_{0w}$ .  $\square$

## Appendix C: Discontinuous Bifurcation

Denote  $E_f^* = (S_{hf}^*, I_{hf}^*, I_{vf}^*)$  be any endemic equilibrium of system (4). Assume that (H1), the conditions of (F1),  $\bar{\alpha}_1(I_{hf2}) > 0$ ,  $\bar{\alpha}_2(I_{hf2}) > 0$  and  $\Delta(I_{hf2}) < 0$  hold. When  $I_{hf}^* < b$ ,  $E_f^* = E_{hf0}$  is stable, and when  $I_{hf}^* > b$ ,  $E_f^* = E_{hf2}$  is unstable. Furthermore, if  $I_{hf}^* = b$ , then there exist a pair of conjugate complex eigenvalues for  $J(E_f^*)$ . Hence, we expect a limit cycle can bifurcate when  $I_{hf}^*$  passes through  $b$ , which is called discontinuous bifurcation (Leine and Nijmeijer 2004; Clarke et al. 2008; Leine and Van Campen 2006) since system (4) is non-smooth at  $I_{hf}^* = b$ . Note that equilibrium  $E_b^* = \left(\frac{d_h N_h - (\mu_1 + r + d_h)b}{d_h}, b, \frac{a\beta_2 N_v b}{a\beta_2 b + d_v N_h}\right)$  for  $I_{hf}^* = b$ .

Let  $J_-(E_b^*)$  and  $J_+(E_b^*)$  denote the left and right Jacobian of system (4) at endemic equilibrium  $E_b^*$ , respectively. Then,

$$J_{\pm}(E_b^*) = \begin{bmatrix} -\beta_3 \frac{I_{hf}^*}{N_h} - a\beta_1 \frac{I_{vf}^*}{N_h} - d_h & -\beta_3 \frac{S_{hf}^*}{N_h} & -a\beta_1 \frac{S_{hf}^*}{N_h} \\ \beta_3 \frac{I_{hf}^*}{N_h} + a\beta_1 \frac{I_{vf}^*}{N_h} & \beta_3 \frac{S_{hf}^*}{N_h} - (\mu_1 + r + d_h) - \mu'_{\pm}(b)b & a\beta_1 \frac{S_{hf}^*}{N_h} \\ 0 & a\beta_2 \frac{(N_v - I_{vf}^*)}{N_h} & -a\beta_2 \frac{I_{hf}^*}{N_h} - d_v \end{bmatrix},$$

where  $(S_{hf}^*, I_{hf}^*, I_{vf}^*) = E_b^*$ ,  $\mu'_+(b) = -\frac{\mu_1 - \mu_0}{2(b-b)}$  and  $\mu'_-(b) = 0$ . It is obvious that  $J_-(E_b^*) \neq J_+(E_b^*)$  when  $I_{hf}^* = b$ . Note  $J_- \triangleq J_-(E_b^*)$  and  $J_+ \triangleq J_+(E_b^*)$ . We have real parts of eigenvalues of  $J_-$  are all negative, and there exists at least one positive real part eigenvalue of  $J_+$ . Then, there exists a jump from  $J_-$  to  $J_+$ .

It is difficult to study the stability of equilibrium  $E_b^*$ . Here, we introduce the smooth approximation system and the generalized Jacobian matrix of Clarke (Leine and Nijmeijer 2004; Clarke et al. 2008; Leine and Van Campen 2006). In our study, the smooth approximation system of (4) is as follows:

$$\begin{cases} \frac{dS_h}{dt} = d_h N_h - a\beta_1 \frac{I_v S_h}{N_h} - \beta_3 \frac{I_h S_h}{N_h} - d_h S_h, \\ \frac{dI_h}{dt} = a\beta_1 \frac{I_v S_h}{N_h} + \beta_3 \frac{I_h S_h}{N_h} - \left( \mu_0 + (\mu_1 - \mu_0) \frac{2(b-b)}{\epsilon I_h + (2-\epsilon)b - 2b} \right) I_h - r I_h - d_h I_h, \\ \frac{dI_v}{dt} = a\beta_2 \frac{I_h (N_v - I_v)}{N_h} - d_v I_v, \end{cases} \quad (39)$$

with  $0 \leq \epsilon \leq 1$ , and the generalized Jacobian matrix of Clarke at  $E_b^*$  is

$$J = \bar{c}o\{J_-, J_+\} = \{\epsilon J_- + (1 - \epsilon)J_+ \mid \epsilon \in [0, 1]\}.$$

Obviously,  $E_b^*$  is endemic equilibrium of system (39). Let  $J(\epsilon) = \epsilon J_- + (1 - \epsilon)J_+$ . Then,  $J(\epsilon)$  is Jacobian matrix at  $E_b^*$  of system (39). The characteristic equation of  $J(\epsilon)$  is as follows:

$$\lambda^3 + \check{\alpha}_1 \lambda^2 + \check{\alpha}_2 \lambda + \check{\alpha}_3 = 0, \quad (40)$$

where

$$\begin{aligned} \check{\alpha}_1 &= \bar{\alpha}_1(b) + \frac{(\mu_1 - \mu_0)(1 - \epsilon)}{2}, \\ \check{\alpha}_2 &= \bar{\alpha}_2(b) + \left( \beta_3 \frac{b}{N_h} + \frac{a\beta_1}{N_h} \frac{a\beta_2 N_v b}{a\beta_2 b + d_v N_h} + d_h + a\beta_2 \frac{b}{N_h} + d_v \right) \frac{(\mu_1 - \mu_0)(1 - \epsilon)}{2}, \\ \check{\alpha}_3 &= \bar{\alpha}_3(b) + \left( \beta_3 \frac{b}{N_h} + \frac{a\beta_1}{N_h} \frac{a\beta_2 N_v b}{a\beta_2 b + d_v N_h} + d_h \right) \left( a\beta_2 \frac{b}{N_h} + d_v \right) \frac{(\mu_1 - \mu_0)(1 - \epsilon)}{2}, \end{aligned}$$

in which  $\bar{\alpha}_i(b) = \bar{\alpha}_i|_{I_h=b}$ ,  $i = 1, 2, 3$ .

When  $\epsilon = 0$ , the real parts of all roots of Eq. (40) are negative. When  $\epsilon = 1$ , there exist a negative real root and the real parts of two roots of Eq. (40) which are positive. We know that  $\check{\alpha}_3 > 0$  always holds which implies 0 is not a root of Eq. (40). Hence, there is a  $0 < \epsilon^* < 1$  such that Eq. (40) has a pair of purely imaginary roots  $\pm i\omega^*$  ( $\omega > 0$ ) when  $\epsilon = \epsilon^*$ . Therefore, the discontinuous Hopf bifurcation (Leine and Nijmeijer 2004) may occur. Now, we tend to find such  $\epsilon^*$ . Substituting  $i\omega$  ( $\omega > 0$ ) into (40) and separating the real and imaginary parts give

$$\begin{cases} \check{\alpha}_2 - \omega^2 = 0, \\ \check{\alpha}_3 - \check{\alpha}_1\omega^2 = 0. \end{cases} \quad (41)$$

Then,  $\check{\alpha}_1\check{\alpha}_2 - \check{\alpha}_3 = 0$ . So, we can get the unique  $\epsilon = \epsilon^*$  and  $\omega = \omega^*$ , where

$$\epsilon^* = 1 - \frac{-A_1 + \sqrt{A_1^2 - 4A_1A_2}}{2A_0} < 1, \quad \omega^* = \sqrt{\check{\alpha}_2}, \quad (42)$$

in which

$$\begin{aligned} A_0 &= \left( \beta_3 \frac{b}{N_h} + \frac{a\beta_1}{N_h} \frac{a\beta_2 N_v b}{a\beta_2 b + d_v N_h} + d_h + a\beta_2 \frac{b}{N_h} + d_v \right) \frac{(\mu_1 - \mu_0)^2}{4}, \\ A_1 &= \left( \beta_3 \frac{b}{N_h} + \frac{a\beta_1}{N_h} \frac{a\beta_2 N_v b}{a\beta_2 b + d_v N_h} + d_h + a\beta_2 \frac{b}{N_h} + d_v \right) \bar{\alpha}_1(b) + \bar{\alpha}_2(b) \\ &\quad - \left( \beta_3 \frac{b}{N_h} + \frac{a\beta_1}{N_h} \frac{a\beta_2 N_v b}{a\beta_2 b + d_v N_h} + d_h \right) \left( a\beta_2 \frac{b}{N_h} + d_v \right), \\ A_2 &= \bar{\alpha}_1(b)\bar{\alpha}_2(b) - \bar{\alpha}_3(b) < 0. \end{aligned}$$

Then,  $(\epsilon^*, \omega^*)$  is a solution of Eq. (40). It implies that  $\pm i\omega^*$  is a pair of purely imaginary roots of Eq. (40) when  $\epsilon = \epsilon^*$  (Fig. 15). we can obtain the following result.

**Theorem 15** Assume that (H1), the conditions of (F1),  $\bar{\alpha}_1(I_{hf2}) > 0$ ,  $\bar{\alpha}_2(I_{hf2}) > 0$ ,  $\Delta(I_{hf2}) < 0$  and  $\frac{-A_1 + \sqrt{A_1^2 - 4A_1A_2}}{2A_0} < 1$  hold. Denote  $E_f^* = (S_{hf}^*, I_{hf}^*, I_{vf}^*)$  be any endemic equilibrium of system (4). When  $I_{hf}^* = b$ , we have the following:

- (C1) The endemic equilibrium  $E_f^*$  of the smooth approximation system (39) of system (4) is stable for all  $0 \leq \epsilon < \epsilon^*$  and unstable for all  $\epsilon^* < \epsilon \leq 1$ .
- (C2) A discontinuous bifurcation occurs at endemic equilibrium  $E_f^*$  of the smooth approximation system (39) of system (4) as  $\epsilon$  increasingly passes through  $\epsilon^*$ . That is, system (39) has a branch of periodic solutions bifurcating from the endemic equilibrium  $E_f^*$ .

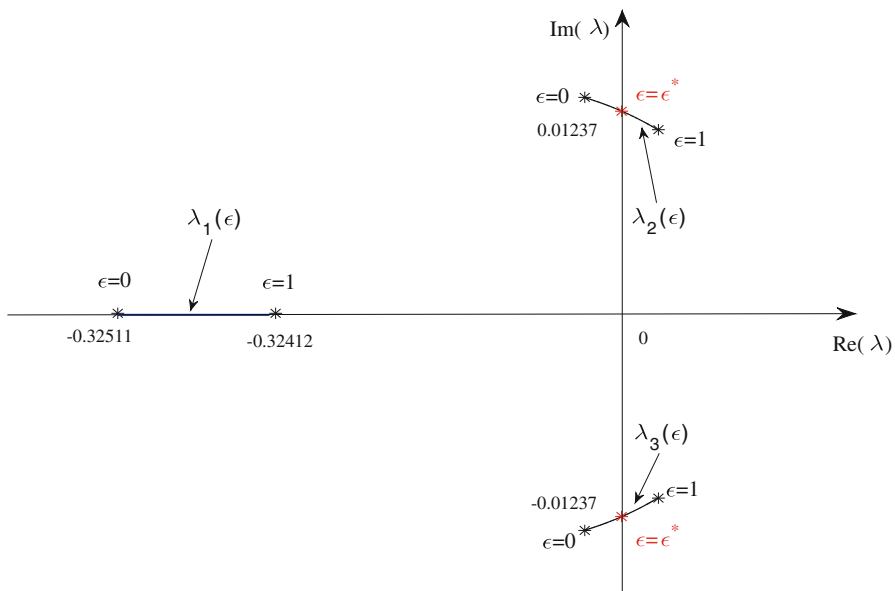


**Fig. 15** Sets of eigenvalues of the generalized Jacobian  $J$ . It has three paths from  $\epsilon = 0$  to  $\epsilon = 1$  with  $\epsilon^* = 0.4892$  and  $\omega^* = 0.01237$ . Here,  $d_v = 0.175$ ,  $\beta_1 = 0.10895$ ,  $\beta_3 = 0.03$ ,  $r = 0.07$ ,  $\mu_0 = 0.08035$ ,  $\mu_1 = 0.081$ , and all other parameters values are shown in Table 2 (Color Figure Online)

## Appendix D: Proof of Theorem 13

**Proof** The translation  $x = S_h - S_h^*$ ,  $y = I_h - I_h^*$ ,  $x = I_v - I_v^*$  brings  $E^*$  to the origin. Expanding the right-hand sides of the resulting system in a Taylor series about the origin, we obtain

$$\begin{cases} \frac{dx}{dt} = -m_2x - m_3y - \frac{a\beta_1 S_h^*}{N_h}z - \frac{\beta_3}{N_h}xy - \frac{a\beta_1}{N_h}xz, \\ \frac{dy}{dt} = (m_2 - d_h)x + (m_3 - m_1)y + \frac{a\beta_1 S_h^*}{N_h}z + \frac{\beta_3}{N_h}xy + \frac{2(\mu_1 - \mu_0)(b - \underline{b})(b - 2\underline{b})}{(I_h^* + b - 2\underline{b})^3}y^2 \\ \quad + \frac{a\beta_1}{N_h}xz + \mathcal{O}(|x, y, z|^3), \\ \frac{dz}{dt} = \frac{d_v I_v^*}{I_h^*}y - m_4z - \frac{a\beta_2}{N_h}yz. \end{cases} \quad (43)$$

The generalized eigenvectors corresponding to  $\lambda = 0$  of Jacobian matrix  $J_{E^*}$  are

$$V_1 = \left( -\frac{m_1 m_4}{d_h}, m_4, \frac{d_v I_v^*}{I_h^*} \right)', \quad V_2 = \left( -\frac{1}{d_h^2} (d_h m_1 + d_h m_4 - m_1 m_4), 1, 0 \right)',$$

which satisfy  $J_{E^*} V_1 = 0$  and  $J_{E^*} V_2 = V_1$ .  $V_3 = \left( -m_3 - \frac{m_2^2}{m_2 - d_h}, m_1 + m_2 - m_3, -\frac{d_v I_v^*}{I_h^*} \right)'$  is the eigenvector of  $\lambda = -\bar{\alpha}_1$ . Let

$$T = (T_{ij})_{3 \times 3} = (V_1, V_2, V_3), \quad (44)$$

then under the non-singular linear transformation

$$(x, y, z)^T = T(x, y, z)^T, \quad (45)$$

then, system (43) becomes

$$\begin{cases} \frac{du_1}{dt} = u_2 + L_{20}u_1^2 + L_{11}u_1u_2 + L_{02}u_2^2 + u_3 \cdot \mathcal{O}(|u_1, u_2|) + \mathcal{O}(|u_1, u_2, u_3|^3), \\ \frac{du_2}{dt} = M_{20}u_1^2 + M_{11}u_1u_2 + M_{02}u_2^2 + u_3 \cdot \mathcal{O}(|u_1, u_2|) + \mathcal{O}(|u_1, u_2, u_3|^3), \\ \frac{du_3}{dt} = -\bar{\alpha}_1u_3 + K_{20}u_1^2 + K_{11}u_1u_2 + K_{02}u_2^2 + u_3 \cdot \mathcal{O}(|u_1, u_2|) + \mathcal{O}(|u_1, u_2, u_3|^3), \end{cases} \quad (46)$$

in which  $L_{20} = \frac{d_v I_v^*}{|T|I_h^*} l_{20}$ ,  $M_{20} = \frac{d_v I_v^*}{|T|I_h^*} m_{20}$ ,  $M_{11} = \frac{d_v I_v^*}{|T|I_h^*} m_{11}$ ,

$$\begin{aligned} L_{11} &= \frac{d_v I_v^*}{|T|I_h^* d_h^4} \left( d_h m_1 + d_h m_4 - m_1 m_4 - d_h^2 \right) \\ &\quad \times \left( \frac{\beta_3 m_1 m_4}{N_h} + (2d_h m_1 + d_h m_4 - m_1 m_4) \left( \frac{\beta_3 m_4}{N_h} + \frac{a\beta_1 d_v I_v^*}{N_h I_h^*} \right) \right) + \frac{d_v I_v^*}{|T|I_h^*} \\ &\quad \times \left[ \left( \frac{1}{d_h^2} (d_h m_1 + d_h m_4 - m_1 m_4) \left( m_1 + m_2 - m_3 - \left( m_3 + \frac{m_2^2}{m_2 - d_h} \right) \right) \right) \frac{a\beta_2}{N_h} \right. \\ &\quad \left. - \frac{m_4}{d_h^2} (d_h m_1 + d_h m_4 - m_1 m_4) \frac{4(\mu_1 - \mu_0)(b - \underline{b})(b - 2\underline{b})}{(I_h^* + b - 2\underline{b})^3} \right], \\ L_{02} &= \frac{d_v I_v^*}{|T|I_h^* d_h^2} \left( d_h m_1 + d_h m_4 - m_1 m_4 \right) \left( \frac{1}{d_h^2} (d_h m_1 + d_h m_4 - m_1 m_4 - d_h^2) \right) \frac{\beta_3}{N_h} \\ &\quad - \frac{2(\mu_1 - \mu_0)(b - \underline{b})(b - 2\underline{b})}{(I_h^* + b - 2\underline{b})^3}, \\ M_{02} &= \frac{d_v I_v^*}{|T|I_h^*} \left[ \frac{1}{d_h^2} (d_h m_1 + d_h m_4 - m_1 m_4) \left( -\frac{m_1 m_4}{d_h} - \frac{m_2^2}{m_2 - d_h} + \bar{\alpha}_1 - m_3 \right) \frac{\beta_3}{N_h} \right. \\ &\quad \left. + \left( \frac{m_1 m_4}{d_h} + \frac{m_2^2}{m_2 - d_h} + m_3 \right) \frac{2(\mu_1 - \mu_0)(b - \underline{b})(b - 2\underline{b})}{(I_h^* + b - 2\underline{b})^3} \right], \\ K_{20} &= L_{20} + \frac{a\beta_2 m_4}{N_h}, \end{aligned}$$

$$K_{11} = L_{11} + \frac{a\beta_2}{N_h},$$

$$K_{02} = L_{02}.$$

We reduce system (46) to a two-dimensional center manifold which corresponds to a pair of simple zero eigenvalues. According to Kuznetsov (1995), there exists a center manifold for system (46) which can be locally be represented as follows

$$W^c = \{(u_1, u_2, u_3) \mid u_3 = F(u_1, u_2), |u_1| < \varepsilon_1, |u_2| < \varepsilon_2, F(0, 0) = 0, DF(0, 0) = 0\}$$

for  $\varepsilon_1$  and  $\varepsilon_2$  sufficiently small. So, we consider the center manifold

$$u_3 = F(u_1, u_2) = s_0 u_1^2 + s_1 u_1 u_2 + s_2 u_2^2 + \mathcal{O}(|u_1, u_2|^3). \quad (47)$$

By putting the center manifold (47) into the third equation of (46), and then by equating powers of  $u_1^2$ ,  $u_1 u_2$  and  $u_2^2$  on both sides, we can calculate the coefficients of the center manifold as follows:

$$s_0 = \frac{K_{20}}{\bar{\alpha}_1}, \quad s_1 = \frac{1}{\bar{\alpha}_1^2}(\bar{\alpha}_1 K_{11} - 2K_{20}), \quad s_2 = \frac{1}{\bar{\alpha}_1^3}(\bar{\alpha}_1^2 K_{02} - \bar{\alpha}_1 K_{11} + 2K_{20}).$$

System (46) restricted to the center manifold is given by

$$\begin{cases} \frac{du_1}{dt} = u_2 + L_{20}u_1^2 + L_{11}u_1u_2 + L_{02}u_2^2 + \mathcal{O}(|u_1, u_2|^3), \\ \frac{du_2}{dt} = M_{20}u_1^2 + M_{11}u_1u_2 + M_{02}u_2^2 + \mathcal{O}(|u_1, u_2|^3). \end{cases} \quad (48)$$

Using the following transformation

$$u_1 = \eta_1 + \frac{1}{2}(L_{11} + M_{02})\eta_1^2 + L_{02}\eta_1\eta_2 + \mathcal{O}(|\eta_1, \eta_2|^3),$$

$$u_2 = \eta_2 - L_{20}\eta_1^2 + M_{02}\eta_1\eta_2 + \mathcal{O}(|\eta_1, \eta_2|^3),$$

then system (48) is topologically equivalent to the normal form (30).  $\square$

## References

- Abdelrazec A, Bélair J, Shan C, Zhu H (2016) Modeling the spread and control of dengue with limited public health resources. *Math Biosci* 271:136–145
- Agusto FB, Bewick S, Fagan WF (2017a) Mathematical model for Zika virus dynamics with sexual transmission route. *Ecol Complex* 29:61–81
- Agusto F, Bewick S, Fagan W (2017b) Mathematical model of Zika virus with vertical transmission. *Infect Dis Model* 2(2):244–267
- Almeida-Filho N (2011) Higher education and health care in Brazil. *The Lancet* 377(9781):1898–1900



- Andraud M, Hens N, Marais C, Beutels P (2011) Dynamic epidemiological models for dengue transmission: a systematic review of structural approaches. *PLoS ONE* 7:3161–3164
- Arbex AK, Bizarro VR, Paletti MT et al (2016) Zika Virus controversies: epidemics as a legacy of mega events? *Health* 8(7):711–722
- Barros AJ, Bastos JL, Dâmaso AH (2011) Catastrophic spending on health care in Brazil: private health insurance does not seem to be the solution. *Cadernos de Saúde Pública* 27:s254–s262
- Brazil Ministry of Health, Zika cases from the Brazil Ministry of Health. <http://portalms.saude.gov.br/boletins-epidemiologicos>
- Camila Z, De MVCA, Pamplona MAL et al (2015) First report of autochthonous transmission of Zika virus in Brazil. *Memórias do Inst Oswaldo Cruz* 110(4):569–572
- Campos GS, Bandeira AC, Sardi SI (2015) Zika virus outbreak, Bahia, Brazil. *Emerg Infect Dis* 21:1885–1886
- Cao-Lormeau VM, Musso D (2014) Emerging arboviruses in the Pacific. *Lancet* 384(9954):1571–1572
- Castillo-Chavez C, Song B (2004) Dynamical models of tuberculosis and their applications. *Math Biosci Eng* 1(2):361–404
- Clarke FH, Ledyaev YS, Stern RJ, Wolenski PR (2008) Nonsmooth analysis and control theory. Springer, Berlin, p 178
- Dick GWA, Kitchen SF, Haddow AJ (1952) Zika virus (I). Isolations and serological specificity. *Trans R Soc Trop Med Hyg* 46(5):509–520
- Diekmann O, Heesterbeek JAP, Metz JA (1990) On the definition and the computation of the basic reproduction ratio  $R_0$  in models for infectious diseases in heterogeneous populations. *J Math Biol* 28(4):365–382
- Duffy MR et al (2009) Zika virus outbreak on Yap Island, federated states of Micronesia. *N Engl J Med* 360:2536–2543
- Froeschl G et al (2017) Long-term kinetics of Zika virus RNA and antibodies in body fluids of a vasectomized traveller returning from Martinique: a case report. *BMC Infect Dis* 17(1):55
- Funk S et al (2016) Comparative analysis of dengue and Zika outbreaks reveals differences by setting and virus. *PLoS Negl Trop Dis* 10(12):e0005173
- Gao D et al (2016) Prevention and control of Zika fever as a mosquito-borne and sexually transmitted disease. *Sci Rep* 6:28070
- Gourinat AC, O'Connor O, Calvez E, Goarant C, Dupont-Rouzeyrol M (2015) Detection of Zika virus in urine. *Emerg Infect Dis* 21(1):84
- Heesterbeek JAP, Roberts MG (2007) The type-reproduction number  $T$  in models for infectious disease control. *Math Biosci* 206(1):3–10
- Hu Z, Teng Z, Jiang H (2012) Stability analysis in a class of discrete SIRS epidemic models. *Nonlinear Anal Real World Appl* 13(5):2017–2033
- Imran M, Usman M, Dur-e-Ahmad M, Khan A (2017) Transmission dynamics of Zika fever: a SEIR based model. *Differ Equ Dyn Syst*. <https://doi.org/10.1007/s12591-017-0374-6>
- Kucharski AJ et al (2016) Transmission dynamics of Zika virus in island populations: a modelling analysis of the 2013–14 French Polynesia outbreak. *PloS Negl Trop Dis* 10(5):e0004726
- Kuznetsov YA (1995) Elements of applied bifurcation theory, applied mathematical sciences. Springer, New York
- Leine RI, Nijmeijer H (2004) Bifurcations of equilibria in non-smooth continuous systems. In: Dynamics and bifurcations of non-smooth mechanical systems. Springer, Berlin, pp 125–176
- Leine RI, Van Campen DH (2006) Bifurcation phenomena in non-smooth dynamical systems. *Eur J Mech A/Solids* 25(4):595–616
- Li G, Zhang Y (2017) Dynamic behaviors of a modified SIR model in epidemic diseases using nonlinear incidence and recovery rates. *PLoS ONE* 12(4):e0175789
- Li C et al (2017) 25-Hydroxycholesterol protects host against Zika virus infection and its associated microcephaly in a mouse model. *Immunity* 46(3):446–456
- Lucchese G, Kanduc D (2016) Zika virus and autoimmunity: from microcephaly to Guillain-Barré syndrome, and beyond. *Autoimmun Rev* 15(8):801–808
- Macdonald G (1952) The analysis of equilibrium in malaria. *Trop Dis Bull* 49:813–829
- Marcondes CB, Ximenes MFF (2016) Zika virus in Brazil and the danger of infestation by *Aedes (Stegomyia)* mosquitoes. *Rev Soc Bras Med Trop* 49:4–10
- Munoz LS, Barreras P, Pardo CA (2016) Zika virus-associated neurological disease in the adult: Guillain-Barré syndrome, encephalitis, and myelitis. *Semin Reprod Med* 34(05):273–279

- Musso D, Roche C, Robin E et al (2015) Potential sexual transmission of Zika virus. *Emerg Infect Dis* 21(2):359
- Petersen LR, Jamieson DJ, Powers AM et al (2016) Zika Virus. *N Engl J Med* 374(16):1552–1563
- Pizza D et al (2016) A model for the risk of microcephaly induced by the Zika virus (ZIKV). *Open J Model Simul* 4(03):109
- Reznik SE, Ashby CR (2017) Sofosbuvir: an antiviral drug with potential efficacy against Zika infection. *Int J Infect Dis* 55:29–30
- Roa M (2016) Zika virus outbreak: reproductive health and rights in Latin America. *Lancet* 387:843–843
- Roberts MG, Heesterbeek JAP (2003) A new method for estimating the effort required to control an infectious disease. *Proc R Soc Lond B Biol Sci* 270(1522):1359–1364
- Ross R (1911) *The prevention of malaria*. John Murray, London
- Saad-Roy CM, Ma J, van den Driessche P (2018) The effect of sexual transmission on Zika virus dynamics. *J Math Biol* 77(6–7):1917–1941
- Sacramento CQ, De Melo GR, De Freitas CS et al (2017) The clinically approved antiviral drug sofosbuvir inhibits Zika virus replication. *Sci Rep* 7:40920
- Sasmal SK, Ghosh I, Huppert A, Chattopadhyay J (2018) Modeling the spread of Zika virus in a stage-structured population: effect of sexual transmission. *Bull Math Biol* 80(11):3038–3067
- Schuler-Faccini L (2016) Possible association between Zika virus infection and microcephaly-Brazil, 2015. *Morb Mort Wkly Rep* 65:59–62
- Shah NH, Patel ZA, Yeolekar BM (2017) Preventions and controls on congenital transmissions of Zika: mathematical analysis. *Appl Math* 8(04):500
- Shan C, Zhu H (2014) Bifurcations and complex dynamics of an SIR model with the impact of the number of hospital beds. *J Differ Equ* 257(5):1662–1688
- Shuai Z, Van den Driessche P (2013) Global stability of infectious disease models using Lyapunov functions. *SIAM J App Math* 73(4):1513–1532
- Tang B, Xiao Y, Wu J (2016) Implication of vaccination against dengue for Zika outbreak. *Sci Rep* 6:35623
- Van den Driessche P, Watmough J (2002) Reproduction numbers and sub-threshold endemic equilibria for compartmental models of disease transmission. *Math Biosci* 180(1):29–48
- Wang W (2006) Backward bifurcation of an epidemic model with treatment. *Math Biosci* 201(1):58–71
- Wang W, Ruan S (2004) Bifurcations in an epidemic model with constant removal rate of the infectives. *J Math Anal Appl* 291(2):775–793
- Wang L, Zhao H (2019) Dynamics analysis of a Zika-dengue co-infection model with dengue vaccine and antibody-dependent enhancement. *Phys A Stat Mech Appl* 522:248–273
- Wang L, Zhao H, Oliva SM, Zhu H (2017) Modeling the transmission and control of Zika in Brazil. *Sci Rep* 7(1):7721
- Wang A, Xiao Y, Zhu H (2018) Dynamics of a Filippov epidemic model with limited hospital beds. *Math Biosci Eng* 15(3):739–764
- Wiratsudakul A, Suparit P, Modchang C (2018) Dynamics of Zika virus outbreaks: an overview of mathematical modeling approaches. *PeerJ* 6:e4526
- World Health Organization (2005–2017) World health statistics
- World Health Organization (2016) Essential medicines and health products. Annual Report
- World Health Organization (WHO) (2016) WHO statement on the first meeting of the International Health Regulations (2005) Emergency Committee on Zika virus and observed increase in neurological disorders and neonatal malformations
- World Health Organization, Case definitions of Zika virus. [http://www.paho.org/hq/index.php?option=com\\_content&view=article&id=11117](http://www.paho.org/hq/index.php?option=com_content&view=article&id=11117)
- Zhang Q et al (2017) Spread of Zika virus in the Americas. *Proc Natl Acad Sci* 114(22):E4334–E4343
- Zmurko J et al (2016) The viral polymerase inhibitor 7-deaza-2'-C-methyladenosine is a potent inhibitor of in vitro Zika virus replication and delays disease progression in a robust mouse infection model. *PLoS Negl Trop Dis* 10(5):e0004695